South Dakota State University
Open PRAIRIE: Open Public Research Access Institutional Repository and Information Exchange

Electronic Theses and Dissertations

1965

Creep Tension Tests on Hastelloy Alloy X Bar, Predicting its Behavior and Applying the Data in a Design Problem

Y. V. S. Rao

Follow this and additional works at: https://openprairie.sdstate.edu/etd

Recommended Citation

Rao, Y. V. S., "Creep Tension Tests on Hastelloy Alloy X Bar, Predicting its Behavior and Applying the Data in a Design Problem" (1965). *Electronic Theses and Dissertations*. 3070.
https://openprairie.sdstate.edu/etd/3070

This Thesis - Open Access is brought to you for free and open access by Open PRAIRIE: Open Public Research Access Institutional Repository and Information Exchange. It has been accepted for inclusion in Electronic Theses and Dissertations by an authorized administrator of Open PRAIRIE: Open Public Research Access Institutional Repository and Information Exchange. For more information, please contact michael.biondo@sdstate.edu.

CREEP TENSION TESTS ON HASTELLOY ALLOY X BMR, PREDICTING ITS BEHAVIOR AND APPLYING THE DATA IN A DESIGN PROBLEM

BY

Y. V. S. RAO

A thesis submitted
in partial fulfillment of the requirements for the
degree Master of Science, Major in Mechanical
Engineering, South Dakota State
University

1965

SOUTH DAKOTA STATE UNIVERSITY LIBRARY

CREEP TENSION TESTS ON HASTELLOY ALLOY X BAR, PREDICTING ITS BEHAVIOR AND APPLYING THE DATA IN A DESIGN PROBLEM

This thesis is approved as a creditable and independent investigation by a candidate for the degree, Master of Science, and is acceptable as meeting the thesis requirements for this degree, but without implying that the conclusions reached by the candidate are necessarily the conclusions of the major department.

Thesis Adviser ✓ Date

Head, Mechanical Engineering Department ✓ Date

ACKNOWLEDGMENTS

It is a great pleasure to me to offer my thanks to Professor Sandfort for his kind help and encouragement in bringing this thesis to this form.

The author wishes to express his sincere appreciation to the former thesis adviser Dr. Huang; Dr. Jannardana Rao, The Minneapolis-Honeywell Regulator Company, Minneapolis, Minnesota; and the staff of the Department of Mechanical Engineering.

The author is also grateful for the generous help of Professor Alfred G. Trump and Mr. Paul Wittkopf who arranged Inter-Library loans and part time work during my research. I am also thankful to Mr. W. J. Pickett, who provided part time work during my stay in Brookings.

The author wishes to thank Pratt & Whitney Aircraft and Union Carbide Corporation for their suggestions and for supplying Hastelloy X bar material for his experiments.

The author is also thankful to Mr. Frank Cosby, Department of English, University of Alabama for proof reading this manuscript.

Finally, the author wishes to thank his wife, Mrs. Rajamma, who encouraged him to go abroad for higher studies.

YVSR

TABLE OF CONTENTS

Page

LIST OF FIGURES

LIST OF TABLES

NOMENCLATURE

ϵ = Creep deformation

ϵ_i = Initial deformation

ϵ_p = Plastic deformation

t = Time

$a, b, K_1, K_2, K_3, K_4, d$ = Constants

τ = Shear stress

G = Shear modulous of elasticity

Creep strain = Creep deformation in inches per inch

$A\bar{t}$ = Average of $\bar{t}$ observations

$A\bar{c}$ = Average of $\bar{c}$ observations

$\bar{t}$ = Log t

$\bar{c}$ = Log c

c = Creep strain

C = Minimum creep rate in in./hr.

S = Stress

n = Number of observations

N = Speed, R.P.M.

Sc = Average tensile stress due to centrifugal forces

A = Annular flow area in sq. in.

γ = Specific weight of the material

M = Bending moment

V = Velocity in ft./sec.

v = Specific volume

g = Gravitational constant

V = Change in velocity

P = Change in pressure

h = Height of the blade

z = Number of blades in a Turbine blade ring

r_t = Radius of the Turbine wheel up to Turbine blade tip

r_m = Radius of the Turbine wheel up to Turbine blade root

r_r = Mean radius of the Turbine wheel

Θ = Angle between the principal and X axis

Z = Modulous of section

Z = Distance measurements in Turbine blades

I_p, I_q, I_y, I_x = Moment of inertia

I_{xy} = Product of inertia

K = Stress concentration factor

f_t = Taper factor

R_v = Ripple factor

L = Length

Σ = Summation sign

$\frac{\partial P}{\partial Q}$ = Partial derivative of P with respect to Q

INTRODUCTION

Creep is a continuing deformation at elevated temperatures under constant stress. Creep data are important in the design of many machine members subjected to high temperatures. Examples of these would be steam and gas turbine components, thermal cracking equipment in oil refineries, jet air-craft, missiles, rockets and mobile reactors.

The second law of thermodynamics shows us that the efficiency of an ideal heat engine can be increased by increasing the temperature of the working fluid. The optimum strength-to-weight ratio is an essential requirement in aircraft structural design. But all these facts bring us the problem of higher creep rates for the same stresses. Few materials at normal temperatures and the remaining at elevated temperatures deform continuously with time under constant loads. So the necessity to investigate the factors influencing the creep and in turn to develop the creep resistant materials is the main concern of a practical engineer.

In some applications, the permissible creep deformations are critical, e.g., allowance for creep is important in turbine blades for proper operation to maintain small clearances between the moving and stationary parts and in others no significance. But the existence of creep, creates the necessity, to know the creep deformations that may occur during the expected life of the machine member.

The creep phenomenon has been known for the last 80 years, but knowledge of the phenomenon has advanced rapidly since World War II, due to more demand for high temperature materials, resulting in today's successful new alloys. Progress has been made in developing the dislocation theory in explaining the creep phenomenon and in obtaining all the data required in design by different techniques and experiments.

Creep deformation can be determined in the laboratory with a testing machine but conducting such tests for the entire life of the machine element is impracticable. So predicting its behavior from short time tests, i.e., 1% of the life time, and extrapolating the data to the entire life of the member is a great achievement in this field.

As we know, the operating characteristics of an original model can be obtained from a small scale model by means of dimensional analysis. Pratt & Whitney Aircraft's Nuclear Operation(1) has been experimenting with lead model testing in order to reduce the heavy financial burden of creep testing of structures. The idea was to have lead creep curves similar to those of the original material in order to obtain direct extrapolation from low temperature lead tests to operating conditions. It is doubtful that we can get consistent results in this way because of poor dimensional control, and other manufacturing

---

(1) Marin, Joseph (Editor), "Materials Engineering Design for High Temperatures," Dept. of Engineering Mechanics, The Pennsylvania State University.

variables involved in a lead model. If at all successful, this would be a great achievement because this would not only reduce the heavy financial burden, but it would also provide all the experimental data within the minimum time.

Cases occur where parts are subjected to combined bending and direct load. For example, turbine blades are subjected to a bending action due to the transverse loading applied by the steam, and to a direct load due to centrifugal force. Parts under eccentric load are also cases in which a cross section is subjected to both bending and direct load. Under creep conditions, parts subjected to this combined straining action when the predominant action is bending are much more favorably stressed than would be the case if the material were elastic; and when the predominant action is a direct load the stress conditions will approach those for elastic conditions. So analyzing the forces acting on a machine element is an important step in a design problem.

CREEP PHENOMENON

At ordinary temperatures the extension that appears on loading disappears after the load is removed provided the load is not sufficiently great to produce failure. At elevated temperatures, the extension continues with time if the stress is maintained constant even under low stress. In other words materials subjected to a constant stress at elevated temperatures deform continuously with time, and the behavior under these conditions is different from the behavior at normal temperatures. This continuous deformation with time is called creep. Creep can take place at any temperature above absolute zero. It seems creep of Cadmium has been observed at temperatures as low as 1.2°K, but from a practical point of view, we consider creep as significant only at higher temperatures and neglect the small creep strains at low temperatures.

Creep Characteristic Curves

Thurston,[2] an American Mechanical Engineer, was the first person to present creep data in the form of a creep - time curve, and this is still well known as the creep characteristic curve. This can be divided into four distinct stages as shown in Figure I. They are as follows:

---

(2) Finnie, I. and Heller, W. R., "Creep of Engineering Materials," McGraw Hill Book Co., Inc., New York, 1959.

(1) First stage: Total deformation is partially elastic which is also known as time independent deformation or static elasticity and partly plastic.

(2) Second stage: Here the creep rate decreases with time. This is known as transient or primary creep, $\frac{d\epsilon}{dt} < 0$. This shows the effect of strain hardening.

(3) Third stage: Here the creep rate is minimum and constant ($\frac{d\epsilon}{dt} = 0$) indicating that the effect of strain hardening is counterbalanced by the annealing influence of high temperature. This is known as secondary creep.

(4) Fourth or final stage: Creep rate increases until fracture occurs due to decrease in cross sectional area. This is also known as tertiary creep ($\frac{d\epsilon}{dt} > 0$).

From the measurements made in long time tension tests, a family of creep - time curves can be obtained for various stress levels at constant temperature. The final stage of the creep curve cannot be seen for low stresses and temperatures during the conventional creep test periods. In the second stage, the strengthening due to strain hardening predominates. Thus the creep rate decreases with time until the minimum or constant creep rate occurs, whereas in the final stage, the weakening due to the annealing influence predominates, and thus the creep rate increases until the fracture takes place.

If large creep deformations are permissible and steady state creep is well established, then the design can be based on steady state creep alone. Otherwise, the initial partly elastic and partly plastic and transient creep should be taken into account. Various authors proposed different empirical expressions to represent constant stress data. The earliest work was done by Andrade[3] who verified the experimental results by means of an empirical relation, $L = L_o(1 + at^{1/3})e^{bt}$ where L_o is the length immediately after loading, L is the length at any time t, and a&b are experimental constants.

Finnie and Heller[4] proposed,

$$\epsilon = \epsilon_o + \sum_{\substack{i=1 \\ o < mi < 1}} a_i t^{mi} + \sum_{\substack{j=1 \\ mj > 1}} bjt^{mj}$$

where ϵ_o is the instantaneous deformation. It seems to be the best fit for creep - time curve since there are many constants involved in this expression. This is the most general expression.

McVetty,[5] Weaver,[6] and Sturm,[7] used different expressions, but these are all complicated because of the fact that the creep - time curve must be available for each stress.

---

[3] Andrade E.N.dac., "The Viscous Flow in Metals and Allied Phenomena," Proceedings of Royal Society (London), Vol. 84, p. 1, 1910.

[4] Finnie and Heller, op. cit., pp. 10.

[5] McVetty, P. G., "Factors Affecting the Choice of Working Stresses for High Temperature Service," Trans. of A.S.M.E., Vol. 55 (1933), p. 99.

[6] Weaver, S. H., "The Creep and Stability of Steels at Constant Stress and Temperature," Trans. A.S.M.E., Vol. 58 (1936), pp. 745-751.

[7] Sturm, R. G., Dumont, C., and Howell, F. M., "A Method of Analyzing Creep Data," Trans. of A.S.M.E., Vol. 58 (1936), pp. 62-67.

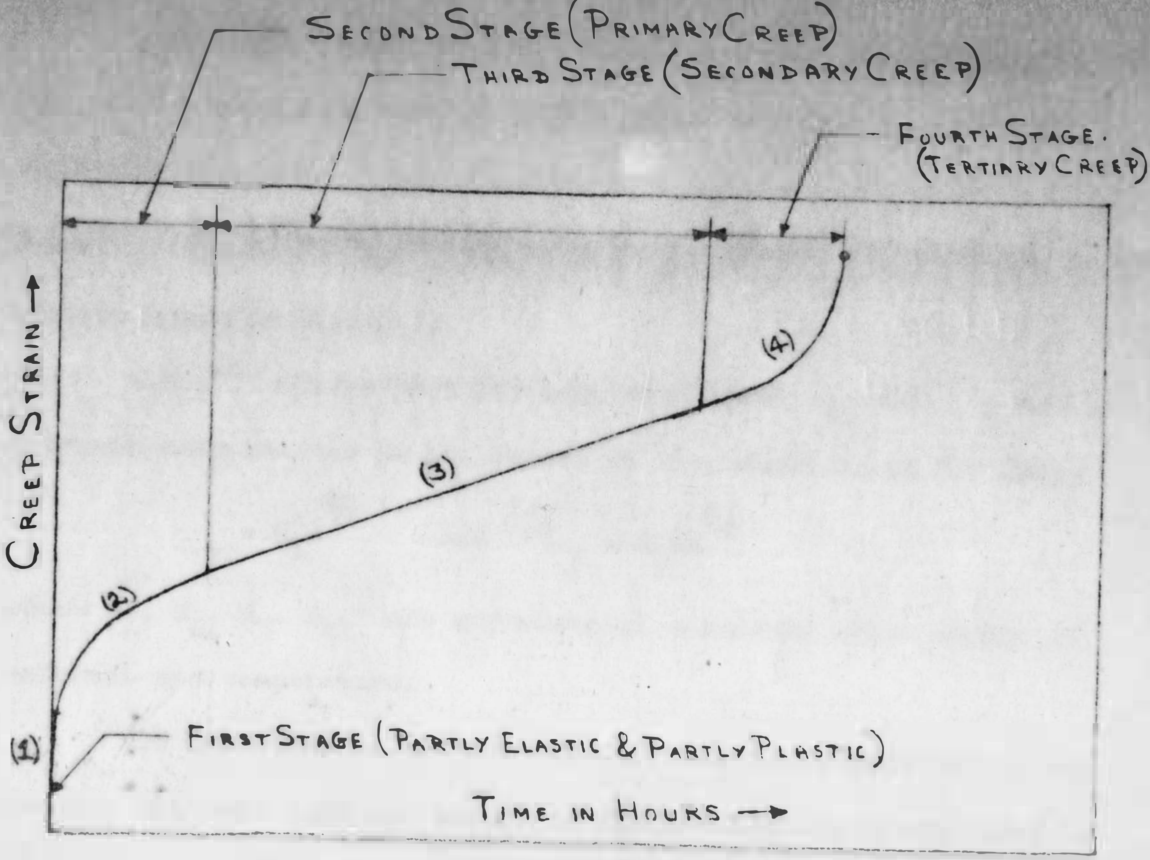

FIGURE I. CREEP CHARACTERISTIC CURVE SHOWING VARIOUS STAGES.

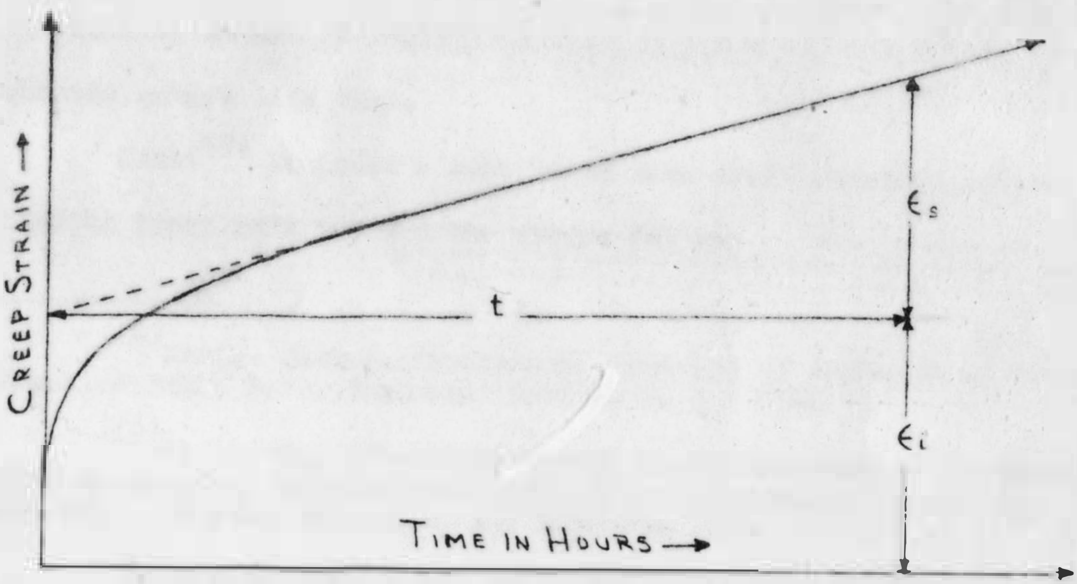

FIGURE II. CREEP-TIME RELATION FOR A CONSTANT STRESS DATA.

Regarding creep - stress - time relations, the modified log - log method takes into account both initial strain (ϵ_i) and time dependent strain (ϵ_p) as follows:

$$\epsilon = \epsilon_i + \epsilon_p$$

This is shown in Figure II.

Marin[8] states that for many materials ϵ_o and ϵ_p can be approximately related to the stress by the equations of the form,

$$\epsilon_o = K_1 S^{K_2} \quad \text{and} \quad \epsilon_p = K_3 t S^{K_4}$$

where K_1, K_2, K_3, K_4,* are experimental constants which depend on material and temperature.

The log - log method neglects the initial strain and is the easiest and most suitable method in calculating the creep rates in turbine blades where the creep deformation would not exceed 0.001 inch per inch during the expected life time of the turbine. In this case the initial strain is negligible when compared to time dependent creep for the entire life time.

Nadai[9] proposed a hyperbolic sine creep relation between minimum creep rate (C) and the stress (S) as

---

[8] Marin, Joseph, "Mechanical Behavior of Engineering Materials," Prentice Hall, Inc., Englewood Cliffs, N. J., 1962.

[9] Nadai, A., "The Influence of Time Upon Creep - The Hyperbolic Sine Creep Law," Stephen Timoshenko 60th Anniversary Volume, The Macmillan Company, New York, pp. 155-171, 1938.

*K_1, K_2, K_3, K_4, a, b, and d are constants and they do not have the same value in each and every expression.

$$C = K_1 \sinh \frac{S}{d}$$

where K_1 and d are experimental constants.

There is no proof to show that the predicted values with the help of these empirical relations represents actual values for the period not covered by the test data, even if these empirical relations fit well the test data.

Atomistic Theory

The data obtained on one material in different laboratories[(10)] show the scatter of creep data (Figure III). So the load-carrying ability determined on the simple tension creep data by empirical and semi-empirical methods may not be satisfactory. The results obtained from the creep tests and further development of stronger materials can be expected with confidence only with an understanding of micromechanism of deformation, microstructure, and by considering the dependence of flow rates of these materials on stress, time, and temperature.

The progress that has been made in understanding creep phenomena is largely due to the atomistic theory. Theoretical strength of a perfect single crystal is approximately equal to $G/2\pi$, where G is the shear modulus of elasticity. But most of the single real crystals have very low yield strengths of 10^{-3} to 10^{-4} of this value. This discrepancy is due to the presence and motion of imperfections that exist in

---

[(10)] Clark, C. L., "Cooperative Creep Tests on 0.35C Steel K20 at 850°F and 7500 psi," Trans. of A.S.M.E., Vol. 59, pp. 439-440, 1937.

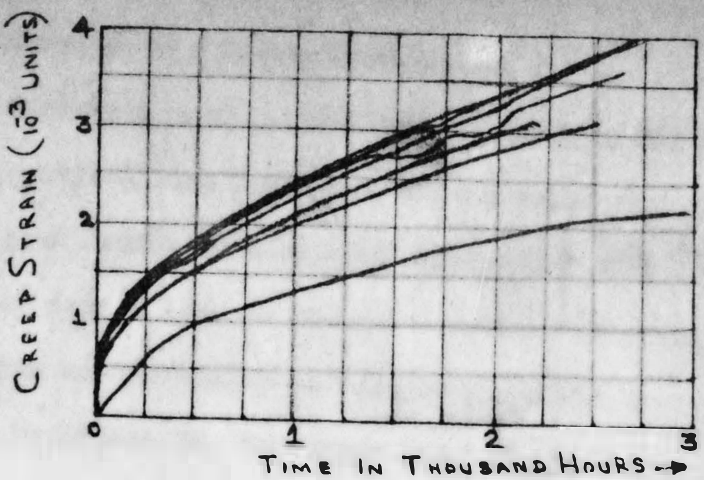

FIGURE III. SPREAD OF CREEP DATA OBTAINED ON THE SAME STEEL AT VARIOUS LABORATORIES.

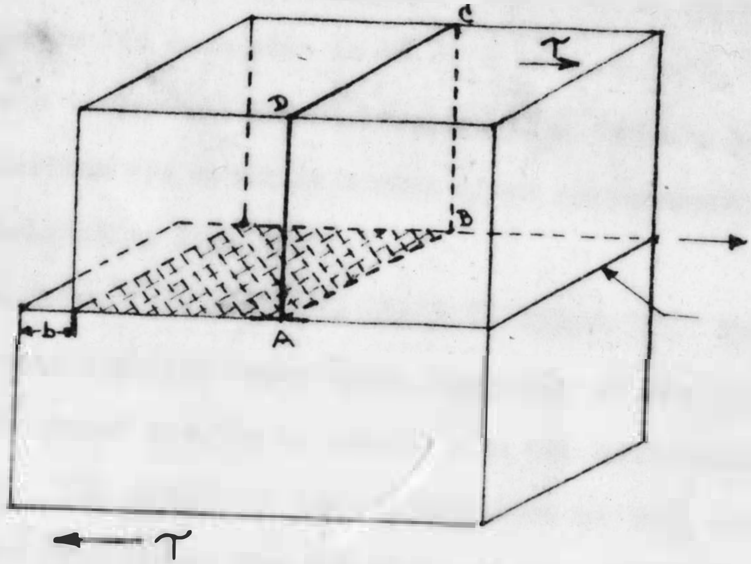

FIGURE IV. EDGE DISLOCATION (3-DIMENSIONAL VIEW) real crystals. The concept of dislocation imperfections has come to explain the difference between the observed strengths of crystals and those calculated on a theoretical basis.

A dislocation is a line imperfection in the regular array of atoms of a crystalline lattice. This demarks the slipped region from the unslipped region in a crystal undergoing slip. Hence dislocation must either form a loop or end on a surface of a crystal. These line dislocations may be either an edge dislocation or a screw dislocation. Referring to Figure IV, the upper half of the crystal has been made to slip by one atomic spacing b in a crystal at the left hand side, and the line AB is known as an edge dislocation with a Burger's vector b in a slip direction. This defect can be visualized in the atomistic picture shown in Figure V in which the Burger's circuit closes everywhere except around the dislocation. This can be checked by going two atom distances for each step (c to d, d to e, e to f, and f to g). The Burger's vector and the dislocation line defines the slip plane. The edge dislocation moves in a slip plane perpendicular to the direction of dislocation line AB.

The screw dislocation is shown in Figure VI. From this figure it can be seen that the upper right hand side of the crystal is made to move one atomic spacing b, relative to the lower right hand side of the crystal. The motion of this dislocation is in a direction normal to AB on the slip plane, but the plane of the screw dislocation is parallel to the Burger's vector.

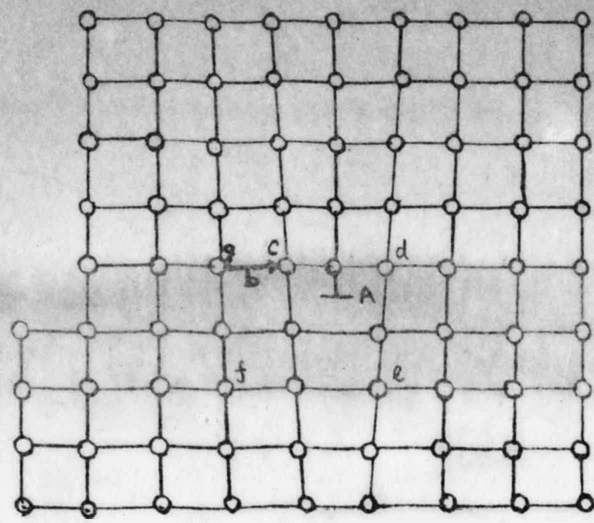

FIGURE V. ATOMISTIC PICTURE OF AN EDGE DISLOCATION (2-DIMENSIONAL VIEW)

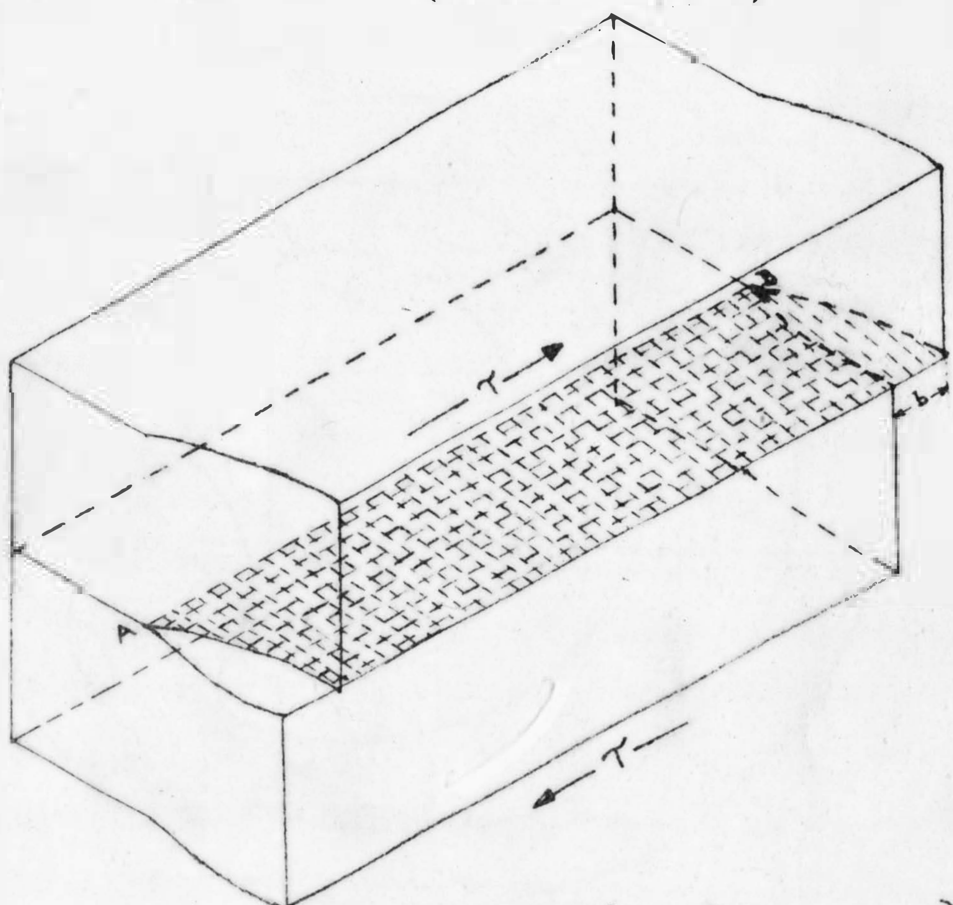

FIGURE VI. SCREW DISLOCATION (3-DIMENSIONAL VIEW)

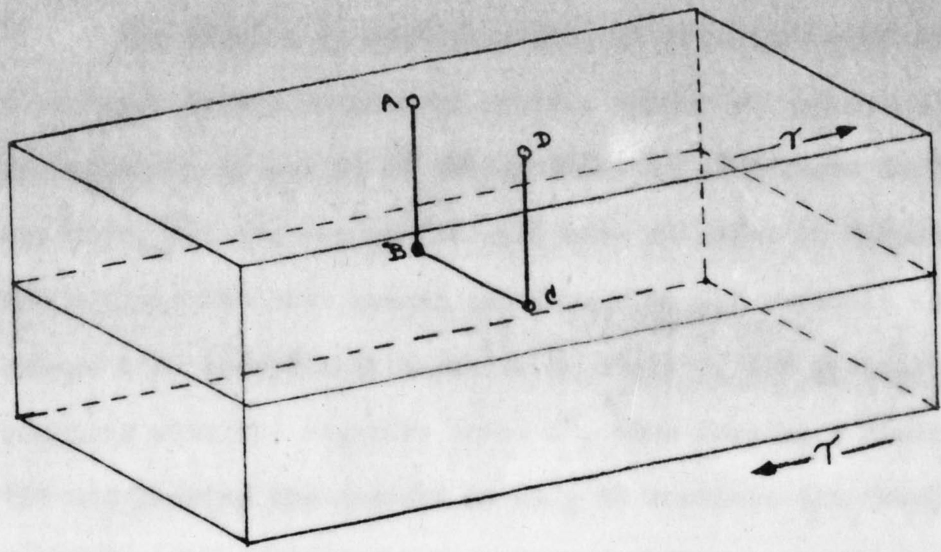

Figure VII. Dislocation In A Crystal.

Figure VIII. Frank-Read Source In Plan View.

173882 SOUTH DAKOTA STATE UNIVERSITY LIBRARY

The problem of multiplication of these dislocations can be visualized from a Frank-Read source. Under an applied shear stress, the segments AB and CD of the dislocation ABCD shown in Figure VII will not move, but the segment BC will move as shown in Figure VIII since the dislocation must remain continuous in the crystal. When the loop swings back upon itself as shown by stage e, the positive screw S^+ combines with the negative screw S^-, thus forming a dislocation ring 'f' and leaving the segment BC at g to continue the former process i.e., grinding out continuously a series of dislocation rings from a single source. When the back stresses on these Frank-Read sources due to the piled up arrays of dislocations are higher, the source ceases to function. The time dependent deformation following this condition is known as creep.

Referring to Figure IV, when the back force on an edge dislocation is equal and opposite to the force due to the applied stress, the further motion of an edge dislocation is stopped, but the vacancies present in the crystal wander about, exchanging their positions with adjacent atoms. These vacancies increase as the temperature increases. Under appropriate conditions, vacancies will exchange their positions with the lowest atom in the half plane of an edge dislocation forcing the dislocation to climb to higher slip planes due to the continuation of this exchange process. When the back stresses are lower, these dislocations will act as new Frank-Read sources and new dislocation loops will be formed. Otherwise the edge dislocation will climb downward by

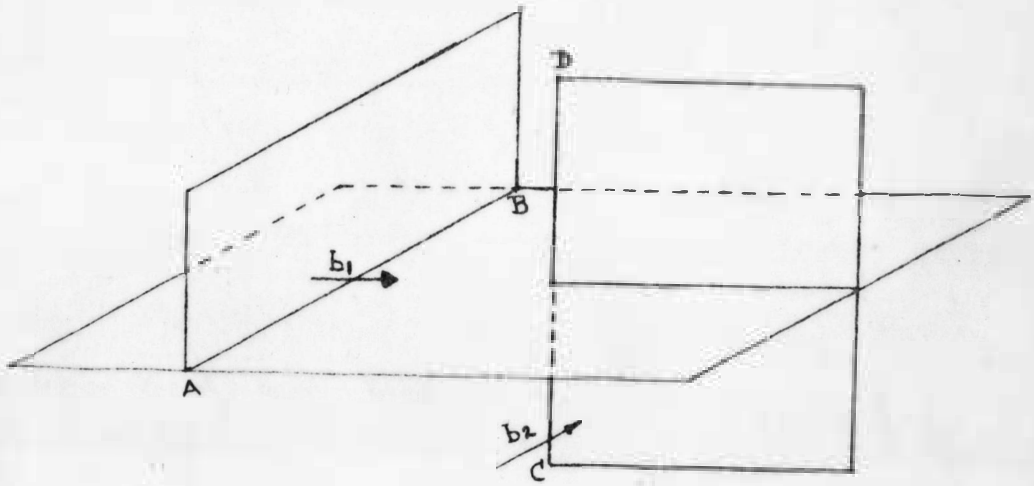

(a) BEFORE INTERSECTION.

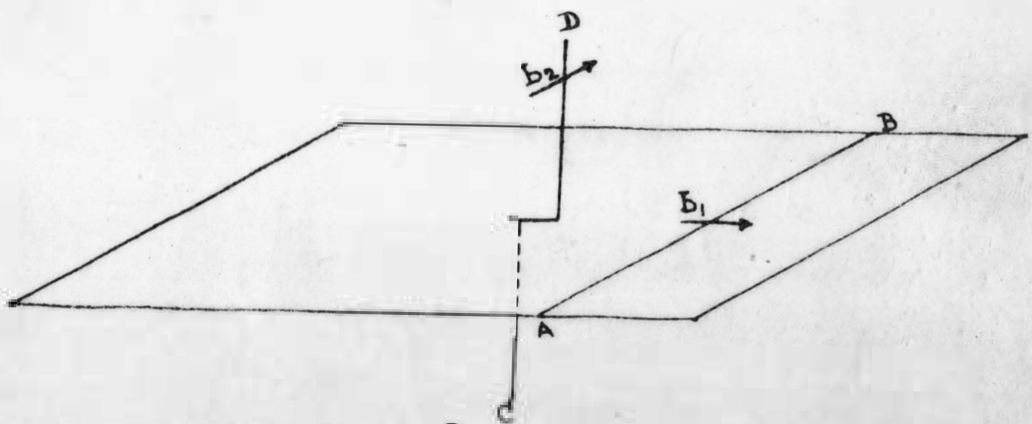

(b) AFTER INTERSECTION.

FIGURE IX. INTERSECTION OF TWO EDGE DISLOCATIONS.

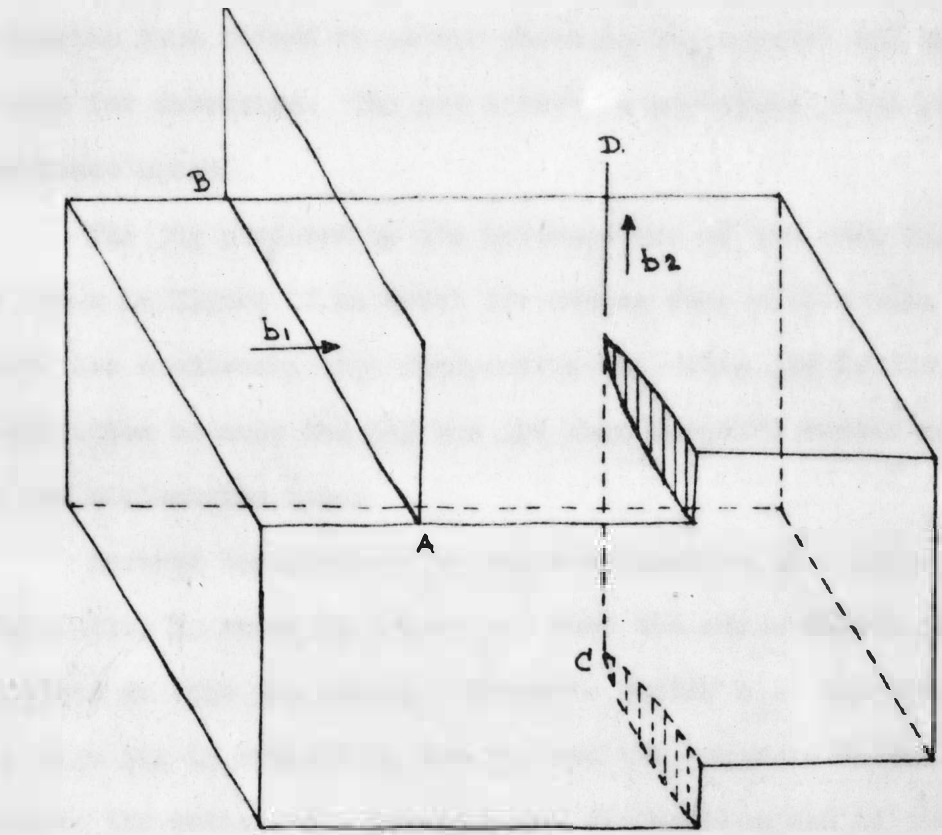

(a) Before Intersection.

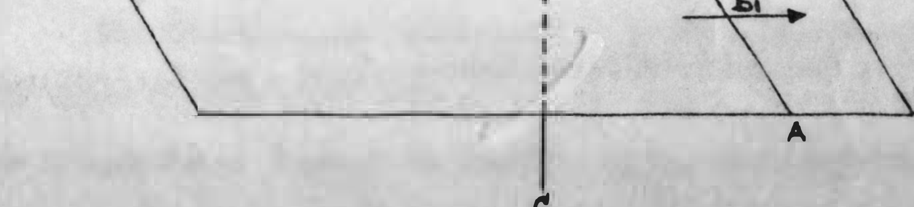

(b) After Intersection

Figure X. Intersection Of An Edge With A Screw Dislocation.

adding adjacent atoms to the bottom of the half plane allowing the vacancies thus formed to wander about in the crystal and thus act as a sink for vacancies. The net effect is continued climb resulting in continued creep.

The jog produced by the intersection of two edge dislocations is shown in Figure IX in which the moving edge dislocation AB intersects the stationary edge dislocation CD. This jog is also an edge jog dislocation because the jog has the same Burger's vector as the rest of the dislocation line.

Another jog produced by the intersection of a screw and an edge dislocation is shown in Figure X. Here the screw dislocation also acquires an edge jog having a Burger's vector b_1. The slip plane of the edge jog is defined by the jog and the Burger's vector. If we observe the motion of a jogged screw dislocation and if the screw moves as shown in Figure XI, the edge jog travels along, moving perpendicular to its slip plane. This will occur only when the edge jog climbs by leaving there a trail of vacancies or interstitial atoms. These vacancies will be filled up by diffusion due to high temperatures. Thus, climb in this way may contribute to continued high temperature creep.

The theory is not sufficient to predict the time laws for creep. The three factors which will affect the creep rate are time, stress and temperature. Even if we control stress and temperature as constant, the time dependency of creep is not sufficient to find the

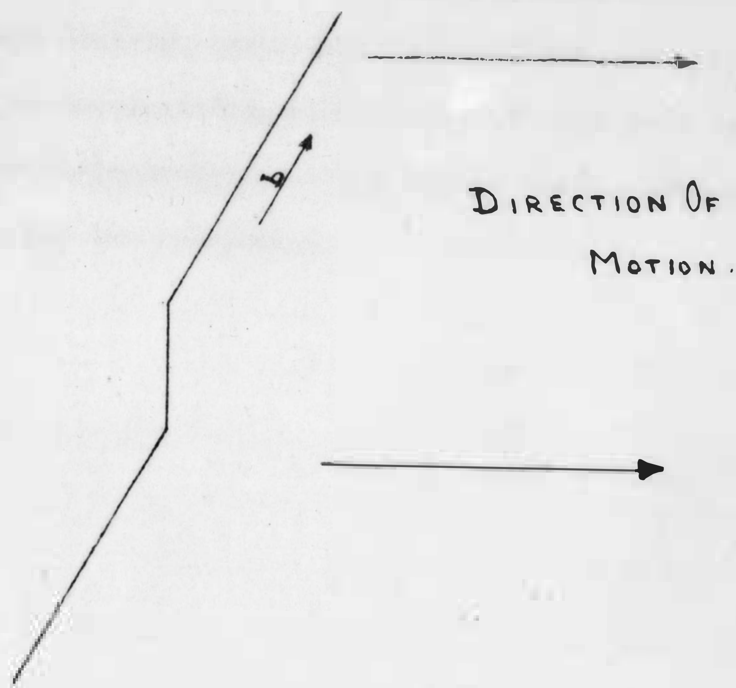

Figure XI. Motion Of A Screw Dislocation With An Edge Jog.

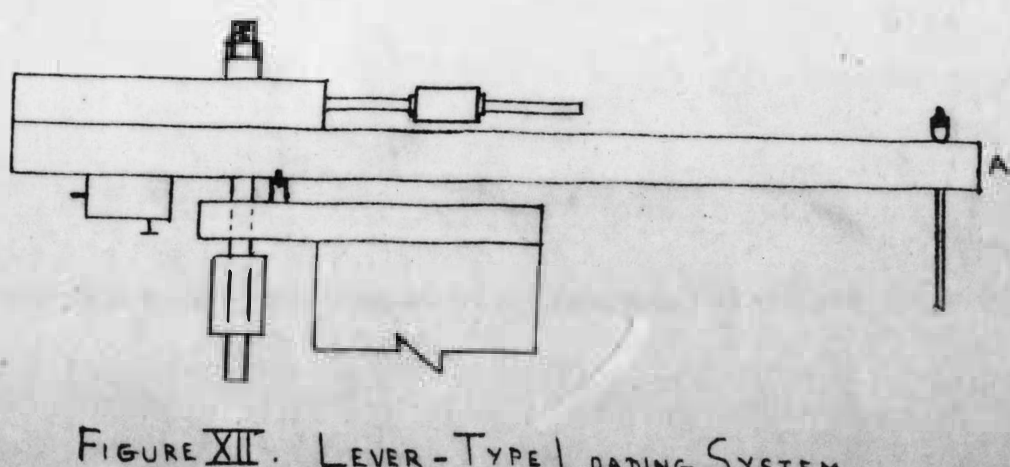

Figure XII. Lever-Type Loading System.

mechanism of creep. Also the effect of other variables like grain size, lattice defects, machining, small differences in chemical composition due to manufacturing inconsistencies and heat treatment processes on the material contributes to the difficulty in arriving at the general expressions for the creep rate.

EXPERIMENTAL STUDIES

Object

The requirements for using metal at elevated temperatures have emphasized the need for securing reliable information about creep under high temperature conditions. Experimental studies serve as a basis for selection of the most suitable metal when there are many metals available which satisfy other design requirements except creep. Experimental studies are also required to extrapolate the data for the entire life time of the machine member to be designed for high temperature service. These experimental studies also help in studying the behavior of the material at various stages with the help of a set of curves obtained as shown in Figure I. With these experimental data as shown in Figure XVI, the interpolation of minimum creep rates for any other stress not covered in these experiments can be determined at that particular temperature from Figure XVIII.

In this creep tension test, a specimen was heated to the desired temperature, a constant load was applied by a lever type loading shown in Figure XII and the resulting slow extension was measured periodically. The creep test has been standardized by the American Society for Testing Materials[11] up to a certain extent. These standards

---

[11] American Society for Testing Materials, "Conducting of Long Time Tension Tests of Metallic Materials," A.S.T.M. Standards, Part 1, Metals, 1958.

specify dimensions of specimens, methods of measuring loads, extensions and temperatures and also methods of reporting these results.

Requisites

The basic requisites for long time creep tension tests are the basic frame assembly having a provision for mounting the specimen and applying a load uniaxially, and other associated components to maintain the load constant. A furnace is necessary to heat the specimen to the desired temperature. An optical system such as a creep microscope or some other automatic device is needed to measure the extension periodically. Since the temperature effect on creep is very significant, a temperature controller is also required. In addition to these accessories, a thermocouple wire and a potentiometer are required to measure the temperature along the specimen gauge length. A thermocouple calibrating furnace and a standard thermocouple are required for calibrating thermocouples. An extensometer (two platinum strips moving relative to each other) is required to determine the creep that is taking place during the test period.

Description

The above mentioned requisites and their description are related to the equipment available for long time creep tension tests in the Mechanical Engineering Department at South Dakota State University. The complete literature for operation and maintenance of the creep testing machine is available in the instruction manual for lever type creep testing machine provided by the Baldwin-Lima-Hamilton Corporation (now known as Wiedemann Machine Company).

According to the manual the upper end of a test specimen is attached to the shorter arm of a lever-arm assembly through an upper specimen holder, spherical yoke and cross-head assemblies. The lower end of the specimen is attached to the output shaft of a screw jack through a lower specimen holder and spherical yoke assembly. The screw jack is connected to a gear motor through a clutch assembly. The operation of the gear motor and screw jack is controlled by a leveling switch assembly. The load applied to the specimen depends upon the weights added to the lever-arm assembly and the ratio between the lengths of the shorter and longer arms of the lever-arm assembly.

As the specimen elongates under load, the outer end of the longer arm (A in Figure XII) moves downward. This downward movement of the longer arm of the lever operates a mercury switch (load leveling switch) which in turn closes a power circuit causing the gearmotor to operate the screw jack to move the output shaft downward. This motion transmitted through the specimen, pulls the shorter arm of the lever downward and as the lever pivots about its fulcrum, the longer arm moves upward. When the lever reaches a level position, the load leveling switch opens the power circuit and thus stops the downward movement of the shorter arm. The same process will be repeated whenever the lever arm is not within plus or minus one degree to the horizontal. Whenever the furnace is turned off or the weights are removed one by one, another mercury-type switch (unload leveling switch in the leveling switch assembly) controls the level of the lever by operating the gearmotor to move the screw jack output shaft upward, thus allowing the specimen to contract which in turn permits removal of the remaining weights.

The furnace is of tubular type having an electrical resistance heating element which is designed to operate on 110 volt, 60 cycle, single phase current. This is rated at 1800°F and instructions for operating it are available in the Marshall furnace instruction book. The most important and difficult step in this furnace operation is in controlling the temperature of the specimen within A.S.T.M.[12] specifications, i.e., maintaining within ±3°F at temperatures from 1100 to 1500°F. Also the temperature variation along the gauge length should not exceed more than 3°F. The temperature exerts a great effect on creep strength. The magnitude of periodically observed extension is of the same order as that produced by a change of temperature of 2°F. Because of these reasons the above limits are essential in order to obtain reliable data.

It was observed that the temperature variation was more than the above A.S.T.M. limits, in the Marshall furnace used. There are four

---

[12] American Society for Testing Materials, "Tentative Recommended Practice for Conducting Creep and Time for Rupture Tension Tests of Materials," A.S.T.M. Standards, Part 3, pp. 274, 1961.

binding posts on the furnace shunt panel to permit localized control of the furnace temperature. This is for the purpose of dividing the heating element into three zones as shown in Figure XIII. A resistance wire shunt was added externally between the two middle binding posts and this brought the temperature variation along the specimen gauge length to within the above limits. It may be possible to keep the temperature variation to minimum by adding the external wire shunt resistance by other alternative ways across the windings. The author suggests that any future research worker performing tests with this furnace, experiment by using a shunt by the trial and error method suggested in the Marshall furnace instruction manual, in order to further reduce the temperature variation along the specimen gauge length. There is a furnace temperature control panel on the creep testing machine basic frame assembly. There are two rheostats provided, one on the top and one on the middle winding, in order to vary the temperature along the specimen gauge length. These rheostats alone are not sufficient to obtain the above accuracy.

In order to suppress the variation of furnace temperature from time to time due to the variation in load (i.e., voltage and current), or due to the other conditions, a furnace temperature controller is required. The chromel-alumel control thermocouple which is located in the furnace windings is the sensing device for this controller. The instructions for operating this potentiometer controller are available in the Foxboro instruction book for potentiometer controller. The temperature at which it is desired to control the process is set on the main dial. Any deviation of temperature of the thermocouple from this setting results in a deflection of the galvanometer pointer to either a low or high position on this dial. When it is in low, a depressor bar which descends at regular intervals arrests the galvanometer pointer. When the pointer is on the side or zero position on the dial, the depressor bar descends completely downward. To the extent that the depressor bar moves, the control contacts are positioned to either maximum or minimum heat connections. The combined effect of this galvanometer pointer and depressor bar thus ensures a uniform furnace temperature. An important point to be noted is that the check switch should not be turned to check position until the dry cell is attached to the battery brackets. Adjusting the zero error of the galvanometer and potentiometer circuit must be done once for proper standardizing. The battery must be renewed whenever the standardizing rheostat reaches the arrow marked on the controller.

Since the rate of extension in the creep test is small, of the order of 1 to 10 percent per 1000 hours, a sensitive and most accurate measuring device is required. The extension measuring part of the apparatus consists of two pieces of platinum (welded to the brackets which can be fixed on the shoulders of the specimen by Allen screws) moving relative to each other by sliding one inside the other. This is shown in Figure XV.

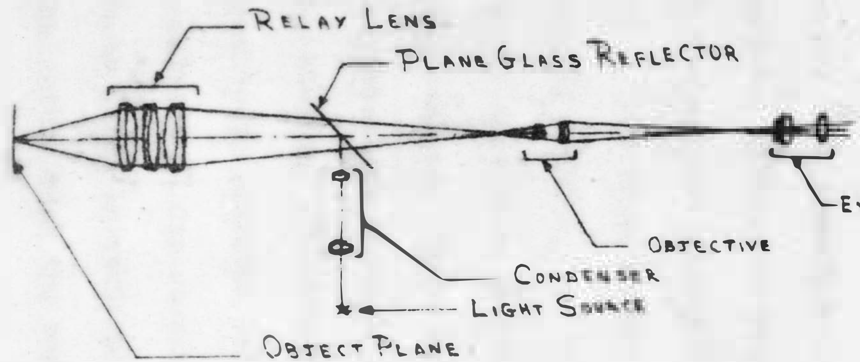

FIGURE XIV. FUNDAMENTALS OF CREEP MICROSCOPE

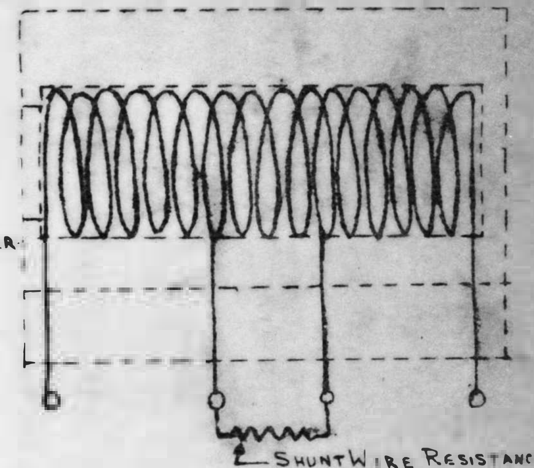

FIGURE XIII. FURNACE ELEMENT WINDING ARRANGEMENT

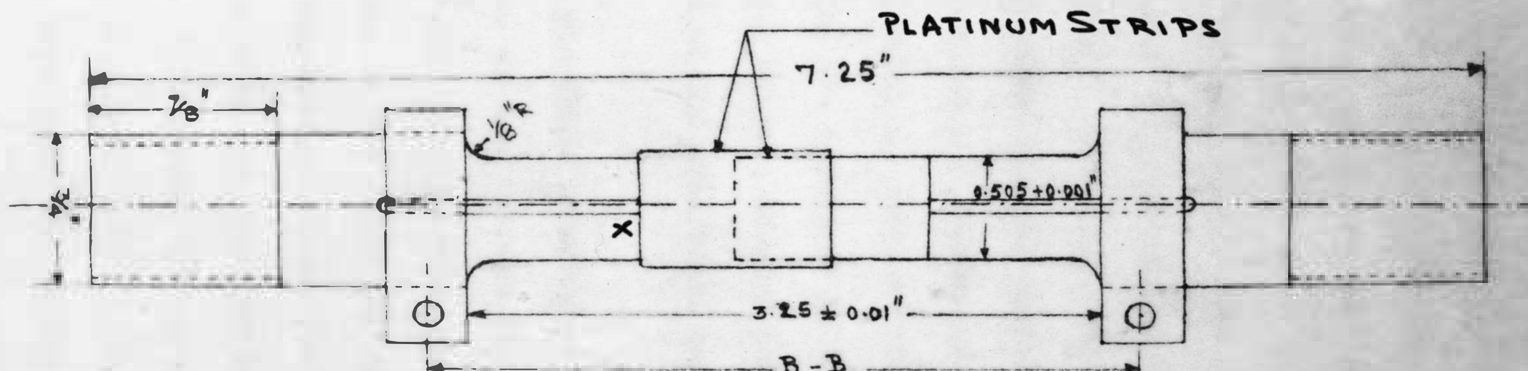

FIGURE XV. SPECIMEN WITH EXTENSOMETER DEVICE

A measuring microscope is always used to measure the creep deformations from time to time. The filar eyepiece micrometer converts a standard microscope into an ordinary measuring instrument of very high precision. In this microscope movable and fixed cross hairs are mounted in the image plane of the objective. The movable cross hairs are mounted on a small carriage which can be moved across the field of view by a fine precision screw. This screw has a divided drum (divided into 100 small divisions) with a knurled knob on top of it for rotating. The fundamentals of the optical system are shown in Figure XIV. The relay lens, without magnifying, projects the image of the object so that it can be picked up by the objective of the microscope. The objective has a magnification of five whereas the filar eyepiece micrometer has a magnification of 10. The total magnification of the optical system is 50.

Two brackets are fixed to the basic frame assembly of the creep testing machine, one on each side of the furnace so that the average of the microscope readings from both sides gives the true axial creep deformations. There is a saw tooth index in the field of view to facilitate counting of whole turns of the divided drum. The motion of the bi-filar cross hairs is such that it can move from one tooth to the next tooth whenever the divided drum or the knurled knob completes one revolution. One revolution of filar drum equals 0.002". Since the saw tooth index is vertical when the filar drum is on top of the microscope, the author took the readings as if reading on a vertical scale, by considering the bottom-most deepest notch as zero, and then counting 1, 2, 3, 4, etc., upwards as the spacing between the successive teeth. Every fifth and tenth notches is cut more deeply than the others for convenience. For example, if the bifilar cross hairs are between 10 and 11, and the divided drum is showing 67, the measurement can be noted as 10.67. Later on, the actual distance between any two reference points can be obtained in inches if we multiply the difference between the two readings by 0.002", since the actual distance between any two teeth is 0.002".

Procedure

Long time creep tension tests are usually carried on to determine the creep deformation of a specimen held at a constant temperature under a predetermined load for a long period of time. These tests are carried out for at least 1 percent of useful service life of the machine member to which the data is to be applied, and 10 percent of the life time where it is feasible. The predetermined tension load which is applied to a specimen held at a constant temperature is constantly maintained as the specimen elongates under load. For this thesis project, the specimen materials used were three bars of Hastelloy alloy X, each 7/8 inches diameter and 8 inches long, obtained from Union Carbide Corporation. The specimen material is a nickel-base alloy and has the chemical composition shown in Appendix A. This is suitable for use in jet engine tail pipes, afterburner components, turbine blades, nozzle vanes, cabin heaters, etc., and is especially useful in furnace applications because it has unusual resistance to oxidizing, reducing and neutral atmospheres. Pratt and Whitney Aircraft authorities suggested that the author conduct creep tests on this Hastelloy X nickel base alloy at 1800°F. Since we experienced some difficulties with the Variac of the power transformer in the furnace electrical connections, it was decided instead to conduct creep tension tests at 1200°F. The specimens were machined in the machine shop to the dimensions shown in Figure XV. Smooth finishing was given by emery cloth to avoid stress raisers.

The lever of the creep testing machine was balanced before starting the test. The lever arm was pivoted about its fulcrum in a 40:1 position.* To balance the lever arm the upper specimen holder was screwed to upper adapter and the weight pan was removed from the weight rod. The counterpoise was now moved until the lever arm balanced. The counterpoise was fixed in this position by lock nuts. When it was balanced properly, the clearance between the top of the top plate and the bottom of the lever was the same at the front and rear of the top plate.

The next step was making and calibrating the thermocouples to measure the temperature along the gauge length of the specimen at frequent intervals. Three thermocouples were made from a 20 B and S

*Putting one pound of weight on a weight pan equals applying 40 pounds of tension load on the specimen. The other ratio, that is possible in this machine is 10:1.

gauge chromel-alumel duplex thermocouple wire. The insulation and other foreign material were scraped off a one inch length of both chromel and alumel wires. The two wires were then bent together without twisting, and the hot junction of the thermocouple was then welded with an oxygen-acetylene torch after applying borax as a flux at the junction. For the operation the oxygen-acetylene torch should be adjusted in between the neutral and slightly oxidizing flame, and the weld should be completed in one pass. For a prospective thermocouple, the diameter of the bead should be approximately equal to three times the diameter of the thermocouple lead wire. Since the thermocouple properties may vary considerably due to the contacts with different materials, they were calibrated in the following way. First the hot junctions of the thermocouple wires were tied to the reduced section of the specimen by a nichrome wire, in such a way that the welded bead would make contact with the specimen but not elsewhere. Asbestos string was then wrapped around the hot junction of the thermocouple, and also along the thermocouple wire which will stay inside the furnace to avoid radiation effects. To calibrate the thermocouples, the specimen to which the hot junctions of thermocouples were attached, and a standard platinum-rhodium thermocouple were suspended so that they stand side by side inside the thermocouple calibrating furnace. Since all thermocouple junctions were not in one place, the distance from each thermocouple junction to the top of the furnace was measured and the standard platinum-rhodium thermocouple was varied accordingly by moving inside or outside depending on which thermocouple was under calibration.

Instead of using the cold junction at 32°F, the reference junction inside the potentiometer was used by compensating the corresponding value to the room temperature. This was accomplished as follows: After adjusting the galvanometer inside the potentiometer for zero error, the potentiometer circuit was then standardized as described in the potentiometer instruction manual. The value which was to be compensated inside the potentiometer was noted from the thermocouple conversion tables, to that particular thermocouple at the room temperature at that time. This value was set on the main dial, the function switch was turned to the reference junction position and the reference junction knob was turned until the galvanometer stood at zero. The potentiometer was thus compensated to the room temperature. To measure the temperature, the function switch was turned to T.C. measure position, the voltage generated by thermoelectric principle was measured and this was converted back into temperature from the thermocouple conversion tables as we did for the cold junctions at 32°F. It is better to use the same potentiometer for both standard platinum-rhodium thermocouple and test thermocouples. The author suggests this procedure in the future because he obtained more accurate data in this way rather than those obtained by using different potentiometers, different cold junctions, and extending the leads of thermocouple wires by other thermocouple wires wherever necessary. The correction readings to the standard platinum-rhodium thermocouple should be taken into account in calibrating these test thermocouples.

Before taking the extension measurements with a creep microscope, it has to be adjusted in such a way that its internal light source and relay lens should focus on the same point. First the eyepiece must be adjusted by moving the eyepiece inside or outside so that the cross hairs are most clearly visible. This can be done by directing the eyepiece to a broad source of illumination such as a sheet of white paper. The microscope is now fixed vertically to a table edge by clamps so that the eyepiece points upwards. A white paper with a cross mark on it is placed under the microscope at 7½" distance (mechanical working distance is 7½") from the bottom end of the microscope. Since the maximum field of view that can be picked up by this microscope is 0.08" in diameter, the cross mark may not be visible through the microscope. The following technique was used to avoid this difficulty so that the center of the cross mark would appear approximately at the center of the image plane. The technique is as follows. If we focus the flash light through the eyepiece of the microscope, this beam of light must converge to a single point source on the white paper, which is at the mechanical working distance of 7½". Whether the mechanical working distance set up is 7½" or not can be checked by loosening the focusing screw on the microscope; then the microscope may be moved up or down so that the cross mark will be clearly visible, and then the focusing screw is tightened in this position. After this is done, the internal light source is adjusted by moving the bulb around inside the illuminator housing, so that the image of the cross mark can be seen clearly and the bulb is fixed in this position by tightening the illuminator clamp screws. Now the microscope is ready for extension measurements.

When all the above equipment was brought to the proper form by various adjustments, the actual creep test was next started. The test thermocouples were calibrated before attaching to the specimen. The extensometer brackets were next fixed to the shoulders of the specimen as shown in Figure XV. The gauge length for this set up was 3.25". The step by step procedure used in installing and loading the specimen is as follows:

(1) After attaching the test thermocouples and extensometers brackets to the specimen, the upper and lower specimen holders are screwed to the specimen. Powdered graphite is applied to the threads for easier disassembly at the end of the test.

(2) The screw jack is operated manually after disengaging from the gearmotor to a position approximately 1" below its maximum upward limit of travel.

(3) The furnace end covers are opened and the furnace is swung on its guide rail away from the rear panel. The furnace power and fuse cable is now plugged into the receptacle provided on the rear panel.

(4) The topmost thermocouple wire and the assembly of specimen holders, specimen, etc., are passed through the furnace from the bottom opening of the furnace towards the top opening until the upper specimen holder can be caught securely from the top of the furnace.

(5) The furnace is now swung towards the rear panel by maintaining the assembly of specimen holders, specimen, etc., at the center of the furnace until the upper specimen holder and lower specimen holder are in line with their corresponding adapters in the sperical yoke assemblies. The furnace can be fixed in that position.

(6) The upper and lower adapters are now screwed on to the specimen holders. All the threaded connections are checked for full thread engagement including those nuts on the spherical yoke assemblies. If the specimen is not at the middle of the furnace, the furnace is moved according to the adjustment needed. In this set up one thermocouple wire is coming out of the furnace from the top opening and the two other thermocouple wires from the bottom opening.

(7) The furnace end covers are closed and kept tight enough by spring action clamps without affecting the movement of specimen holders, after first wrapping the spun glass insulation around the specimen holders where they enter the furnace. This reduces considerably the thermal draft that may occur due to the large temperature differences between the surroundings and the radiation zone of the furnace.

(8) The brackets for mounting the creep microscope at the sides of the furnace are now adjusted so that focusing the microscope through the window glass and thus picking the image of the object from the center of the furnace (i.e., platinum strips in this case) is possible. This can be accomplished only by trial and error by changing the

positions of the bracket and by observing for the image of the object through the eyepiece for each position of the bracket. When the brackets are fixed, they should not be disturbed until the end of the test. It is to be noted that the furnace windings should be calibrated before fixing the specimen to the machine as described on page 24 of this thesis and also according to the instructions of the Marshall furnace instruction book.

(9) The load-unload switch on the leveling switch assembly should be set at "load," and all other switches except load control switch should be set at "off." The load control switch should be set at manual position.

(10) The electric power to the testing machine and to the furnace temperature controller can now be turned on. At this stage, the furnace power switch can be set at "on," and its controls for position and temperature can be adjusted.

(11) Now is the time for calculating the desired load on the weight pan. Since the dimensions of the specimen are standardized, we can find the relation between the weights we are adding to the weight pan and to the stress that will be impressed on the specimen. The reduced section of the specimen under test is 0.505" in diameter, i.e., 0.200377 square inches in cross-sectional area. Since the lever ratio selected is 1:40, one pound of weight on the weight pan implies 40 pounds of tension load on the specimen. In other words, one pound of weight on the weight pan implies $40/0.200377 = 199.624 = 199^{5/8}$ psi stress on a standard specimen used in this creep testing machine. With

this relation we can determine the weights to be added to the weight pan to obtain the desired stress on the specimen. It is to be borne in mind that the small weight pan which weighs two pounds is already on the weight rod and this should be considered in adding the remaining weights to obtain the desired stress. The desired weights are placed on the weight pan such that the slots in the weights are alternately faced in opposite directions which will provide an interlocking action.

(12) The time for the specimen to reach the test temperature varies from 5 to 8 hours depending on the variac setting on the power transformer. In any case, the specimen is brought to the test temperature and maintained there overnight, before the stress is applied. The temperature along the specimen gauge length can now be measured, and if necessary adjusted by means of the fine rheostats provided on the middle and top windings until they show within the American Society for Testing Materials specifications.

(13) To actually load the specimen, the step by step procedure is as follows: The screw jack is operated manually to move the output shaft downward to remove any slack in the assembly of the specimen, the specimen holders, and the adapters, but no load should be imposed on the specimen in this operation. The next step is to switch on the motor power switch. When this is done, the gearmotor can be engaged. The direction control switch can be set at load position. Now the gearmotor will operate the screw jack to move the output shaft downward.

When this motion has brought a small clearance between the top of the spherical yoke assembly and the bottom of the top plate of the basic frame assembly, the load control switch should be set at automatic and the direction control switch should be at the "off" position.

(14) As soon as the lever has leveled and the gearmotor stops, the timer can be started, and then the initial microscope readings should be taken from both sides of the furnace. The most important part of creep tension test is taking creep versus time readings at frequent intervals. Taking creep readings with the help of a creep microscope is the oldest technique and still adopted in some laboratories and industries.

Since the microscope magnified the image of the object fifty times, the lines marked on the platinum strips, fine scratches and other bright specks could be seen in the image plane of the objective. Special jigs and fixtures are required to mark lines on platinum strips. Since such facilities were not available, the author took certain bright specks or fine scratches as the reference points, one on each sheet of platinum near the boundary. It was observed that the best clear image of the object could be seen only when the platinum strip was at right angles to the beam of light or to the axis of the microscope. Since the platinum strips were moving, one inside the other, one strip of platinum was nearer to the microscope than the other strip. Such difference of distances brought the problem of seeing only one strip at a time very clearly, and the other only vaguely. So the microscope had to be focused so that a fair image could be seen on both strips of platinum rather than seeing one clearly and the other one only vaguely. In other words, the microscope must be focused in between the two settings. Since the microscope is so sensitive, the platinum extensometer parts must be made in such a way that these platinum strips should touch each other throughout the test.

The next step is to measure the distance between the reference points. Before measuring this, we have to make sure that the divided drum is at the top of the microscope, so that the saw tooth index stands vertically, and the bifilar eyepiece micrometer is attached firmly to the stainless steel body tube by tightening the screws. The divided drum can be rotated now until the bifilar hair lines encloses one of the reference points. The reading is to be noted as described in the description of the equipment. The divided drum can be turned further until the bifilar hair lines enclose the other reference point. The reading is to be noted in the same way. The difference between the two readings gives the reference distance for our creep measurements. This distance may increase or decrease as the test progresses depending on the relative movement of the platinum strips. Creep measurements must be taken on both sides of the extensometer device to obtain true or axial creep. The above process of taking the readings at the same reference points should be repeated at frequent intervals. The interval depends upon the stress and temperature at which the test is proceeding. When the stress and temperature are high, the readings should be taken four or five times a day in the beginning. If the stress is low, taking the readings two times a day will be sufficient in the beginning. When once the test enters the minimum or constant creep rate state, it does not make any difference whether we take readings once in a day or once in two days.

More consistent readings can be obtained if the focusing can be done at the same place throughout the test, and the readings of the two reference points taken after those reference points are located with the bifilar cross hairs by moving the filar micrometer in the same direction throughout the test. Each reading should be taken two or three times and the mean of these readings recorded as the final reading to improve the accuracy.

Since the temperature effect on creep is very significant, the temperatures along the specimen gauge length should be kept as alike as possible, and the test temperature should be maintained constant. To achieve these benefits, temperature readings of the test thermocouples should be noted in the beginning at least up to one week and corresponding adjustments should be made on the fine rheostats provided on middle and top windings of the furnace. Adjusting first the zero error of the galvanometer in the furnace temperature controller and then potentiometer circuit standardizing must be done once a day to maintain the test temperature constant throughout.

When the stress and temperature are high, the reference points noted in the beginning will move soon out of our field of view. Just before they leave the field of view, two other reference points should be chosen and the same procedure followed. When these two new reference points are chosen, we must take the final readings of the two old reference points and compute the total creep that occurred up to this time. This total creep up to this stage should then be added to the creep of new reference readings.

When enough data has been obtained as explained above, the procedure to be carried out at the end of the test varies depending on whether it was a rupture test, a long time tension test, or a test to find the recovery rate of the test specimen as the load was removed. After noting the final creep and time readings, the corresponding procedure should be followed as explained in the creep testing machine instruction manual. At the end of the test, the diameter of the smallest section on the specimen is measured with a micrometer in order to check the reduction in area.

Results

The object of a creep tension test is to collect creep-time data. All these tests were conducted at a constant temperature of 1200°F. The first test was at 12,500 psi stress level. This test was taken off at 600 hours due to inconsistent creep readings. The main reason for this kind of failure may be due to the fact that the bifilar eyepiece micrometer is not attached firmly to the body of the microscope. Since the stress and temperature are low for this particular material and since there are no clear marks on the platinum strips, the measurement

Table 1. Creep-Time Readings for 12500 Psi Stress Level at 1200°F on Hastelloy X Bar Material

Creep deformation (inches x 10^{-4}) Left	Right	Average	Creep strain (in. per in. x 10^{-4})	Time in hours
*164.74	*17.36			0.3
5.27	5.09	5.18	1.59	9.7
9.61	9.63	9.62	2.96	18.8
6.36	6.18	6.27	1.93	24.0
7.52	7.64	7.58	2.33	33.3
11.40	11.36	11.38	3.50	41.6
13.92	13.64	13.78	4.24	57.1
14.77	14.71	14.74	4.54	68.85
15.54	15.28	15.41	4.75	81.6
10.21	10.95	10.58	3.25	106.3
15.85	14.95	15.40	4.74	128.2
16.86	16.32	16.59	5.10	142.9
20.50	19.98	20.24	6.24	155.8
18.51	18.01	18.26	5.62	178.8
19.78	19.30	19.54	6.01	190.1
22.32	21.58	21.95	6.75	202.3
23.44	22.80	23.12	7.12	220.5
22.88	22.32	22.60	6.95	240.9
23.57	23.17	23.37	7.19	250.3
25.02	24.62	24.82	7.65	274.5
26.33	26.03	26.18	8.05	297.3
29.48	29.12	29.30	9.02	310.6
28.25	27.95	28.10	8.65	329.7
29.86	29.42	29.64	9.13	346.5
31.38	31.02	31.20	9.61	357.8
35.18	34.73	34.95	10.75	370.4
30.83	30.51	30.67	9.45	393.6
45.08	44.12	44.60	13.72	405.8
33.74	33.31	33.52	10.31	429.4
31.53	31.17	31.35	9.65	448.7
33.11	32.65	32.88	10.12	474.6
40.02	39.59	39.80	12.24	501.3
35.23	34.67	34.95	10.75	524.7
36.88	36.33	36.60	11.25	549.6
37.35	36.95	37.15	11.42	600.0

*The distance between the two reference points initially

Table 2. Creep-Time Readings for 25,000 Psi Stress Level at 1200°F on Hastelloy X Bar Material

Units - 10^{-3} inches						
		Cumulative		Creep deformation		
Left	Right	Left (L_T)	Right (R_T)	$= \frac{L_T + R_T}{2}$	Creep strain	Time in hours
17.38	2.64					0.3
16.42	1.73	0.96	0.91	0.935	0.288	10.6
15.80	1.03	1.58	1.61	1.595	0.491	23.0
14.57	- 0.16	2.81	2.80	2.805	0.863	34.9
13.56	- 1.21	3.82	3.85	3.835	1.180	45.7
11.80	- 2.81	5.58	5.45	5.515	1.697	57.2
9.80	- 4.87	7.58	7.51	7.545	2.321	71.7
8.36	- 6.27	9.02	8.91	8.965	2.758	83.8
6.33	- 8.34	11.05	10.98	11.015	3.389	94.3
4.06	-10.42	13.32	13.06	13.190	4.060	107.6
2.40	-12.13	14.98	14.77	14.875	4.580	118.8
0.41	-13.89	16.97	16.53	16.750	5.150	130.4
- 1.49	-15.57	18.87	18.21	18.540	5.700	142.7
- 3.18	-17.49	20.56	20.13	20.345	6.180	154.7
- 4.80	-19.04	22.18	21.68	21.93	6.75	166.6
- 6.86	-21.02	24.24	23.66	23.95	7.37	178.8
- 8.84	-22.96	26.22	25.60	25.91	7.97	190.7
-10.41	-24.69	27.79	27.33	27.56	8.48	203.0
-11.84	-26.43	29.22	29.07	29.145	8.97	215.0
-13.24	-27.98	30.62	30.62	30.62	9.42	226.8
-14.76	-29.55	32.14	32.19	32.165	9.90	238.8
-16.30	-30.85	33.68	33.49	33.585	10.33	251.3
-17.80	-31.96	35.18	34.60	34.89	10.73	263.2
-19.50	-34.15	36.88	36.79	36.835	11.33	275.0
-20.94	-35.82	38.32	38.46	38.39	11.81	287.2
-22.42	-36.67	39.80	39.31	39.555	12.17	298.8
-23.64	-38.44	41.02	41.08	41.05	12.63	310.9
-24.66	-39.21	42.04	41.85	41.945	12.91	321.4
-26.72	-40.68	44.10	43.32	43.71	13.45	334.8
19.81						
18.73	-42.14	45.18	44.78	44.98	13.84	346.0
	12.49					
17.11	11.21	46.80	46.06	46.43	14.29	358.7
15.89	9.80	48.02	47.47	47.745	14.69	370.7
14.98	8.78	48.93	48.49	48.71	14.99	381.8
13.62	7.47	50.29	49.80	50.045	15.40	394.8
12.40	6.47	51.51	50.80	51.155	15.74	407.0

Table 2. (Continued)

Units - 10^{-3} inches						Time in hours
		Cumulative				
Left	Right	Left (L_T)	Right (R_T)	Creep deformation $= \frac{L_T + R_T}{2}$	Creep strain	
11.40	5.23	52.51	52.04	52.275	16.08	419.0
10.18	4.20	53.73	53.07	53.40	16.43	430.0
9.18	2.80	54.73	54.47	54.60	16.80	442.6
7.90	1.66	56.01	55.61	55.81	17.17	454.5
6.91	0.67	57.00	56.60	56.80	17.48	466.0
5.66	- 0.32	58.25	57.59	57.92	17.82	478.9
4.57	- 1.34	59.34	58.61	58.975	18.15	491.1
3.67	- 2.43	60.24	59.70	59.97	18.45	502.6
2.60	- 3.45	61.31	60.72	61.015	18.77	514.9
1.54	- 4.51	62.37	61.78	62.075	19.10	526.6
0.49	- 5.52	63.42	62.79	63.105	19.42	539.2
- 0.49	- 6.32	64.40	63.58	63.99	19.69	551.0
- 1.61	- 7.65	65.52	64.92	65.22	20.07	562.9
- 2.71	- 8.63	66.62	65.90	66.26	20.39	574.4
- 3.83	- 9.79	67.74	67.06	67.40	20.74	587.4
- 4.58	-10.57	68.49	67.84	68.165	20.97	597.5
- 5.68	-11.95	69.59	69.22	69.405	21.35	611.1
- 6.73	-12.76	70.64	70.03	70.335	21.64	621.7
- 7.50	-13.54	71.41	70.81	71.11	21.88	634.0
- 8.83	-14.59	72.74	71.86	72.30	22.25	646.7
- 9.67	-15.72	73.58	72.99	73.285	22.55	659.0
-10.70	-16.55	74.61	73.82	74.215	22.83	671.0
7.16						
6.16	-17.69	75.61	74.96	75.285	23.16	684.2
4.24	-19.40	77.53	76.67	77.10	23.72	706.9
2.26	-21.22	79.51	78.49	79.00	24.30	732.7
0.63	-23.06	81.14	80.33	80.735	24.84	756.0
- 1.09	-24.74	82.86	82.01	82.435	25.36	778.4
- 2.94	-26.50	84.71	83.77	84.24	25.92	802.8
- 4.89	-28.41	86.66	85.68	86.17	26.51	827.0
- 6.37	-30.24	88.14	87.51	87.825	27.02	850.5
4.62						
2.70	-31.86	90.06	89.13	89.595	27.57	875.1
1.00	-33.67	91.76	90.94	91.35	28.18	898.5
- 0.81	-35.31	93.57	92.58	93.07	28.64	922.6
- 2.57	-36.95	95.33	94.22	94.77	29.16	946.2
7.20	-41.67	99.96	98.94	99.45	30.6	1000.0

Table 3(a). Creep-Time Observations for 35,000 Psi Stress Level at 1200°F on Hastelloy X Bar Material

Creep deformation (10^{-3} inch units)										
Left				Right				Average of both sides	Creep strain (10^{-3} units)	Time in hours
(1)	(2)	Average	Total creep	(1)	(2)	Average	Total creep			
8.92	9.04	8.98		11.48	11.64	11.56				0.1
12.82	12.84	12.83	3.85	13.34	13.74	13.55	1.99			8.7
18.18	18.14	18.16	9.18	15.76	15.60	15.68				15.6
23.76	23.86	23.81	14.83	20.68	20.92	20.80				21.6
25.46	25.64	25.55	16.57	21.20	21.24	21.22				27.8
25.32	25.14	25.23	16.25	21.34	21.44	21.39				34.9
24.24	24.22	24.23	15.25	21.54	21.44	21.49				42.7
24.30	24.30	24.30	15.32	21.36	21.40	21.38				47.4
23.96	24.00	23.98	15.00	21.62	21.50	21.56				58.6

Test stopped at 60 hours and started again after refixing the brackets of extensometer device to the shoulders of the specimen.

Table 3(b). Creep-Time Observations for 35,000 Psi Stress Level at 1200°F on Hastelloy X Bar Material

Creep deformation (10^{-3} inch units)										
Left				Right				Average of both sides	Creep strain (10^{-3} units)	Time in hours
(1)	(2)	Average	Total creep	(1)	(2)	Average	Total creep			
19.98	19.92	19.95		19.80	19.82	19.81				0.2
26.72	26.72	26.72	6.77	12.86	12.74	12.80	7.01	6.89	2.0585	6.3
36.18	36.22	36.20	16.25	3.52	3.28	3.40	16.41	16.33	5.0246	14.6
6.62	6.50	6.56								
- 0.18	- 0.30	- 0.24	23.05	- 4.12	- 4.10	- 4.11	23.92	23.485	7.226	20.45
- 9.58	- 9.60	- 9.59	32.40	-12.42	-12.58	-12.50	32.31	32.355	9.955	27.6
-16.70	-16.84	-16.77	39.58	-20.08	-20.08	-20.08	39.89	39.735	12.226	33.6
8.46	8.60	8.53		27.88	27.92	27.90				
0	0	0	48.11	19.62	19.46	19.54	48.25	48.18	14.82	40.4
-13.44	-13.36	-13.40	61.51	5.60	5.70	5.65	62.14	61.825	19.02	51.15
-21.46	-21.40	-21.43	69.54	- 1.72	- 1.78	- 1.75	69.54	69.54	21.40	57.35
-28.60	-28.66	-28.63	76.74	- 9.56	- 9.38	- 9.47	77.26	77.00	23.7	63.6
34.54	34.70	34.62								
25.50	25.58	25.54	85.82	-17.38	-17.62	-17.50	85.29	85.505	26.31	70.4
				36.10	36.22	36.16				
16.46	16.34	16.40	94.96	26.22	26.42	26.32	95.13	95.045	29.24	78.2
6.90	6.88	6.99	104.37	16.98	16.98	16.98	104.47	104.42	32.13	85.9
- 2.44	- 2.52	- 2.48	113.84	7.56	7.52	7.54	113.91	113.875	35.04	93.3
-13.70	-13.48	-13.59	124.95	- 3.90	- 4.06	- 3.98	125.43	125.19	38.52	101.7
-25.32	-25.38	-25.35	136.71	-15.34	-15.52	-15.43	136.88	136.795	42.09	110.2
				47.24	47.04	47.14				
-35.82	-35.60	-35.71	147.07	36.74	36.38	36.56	147.46	147.265	45.31	117.9
37.10	36.92	37.01								
23.18	23.22	23.20	160.88	23.16	23.00	23.08	160.94	160.91	49.51	127.6
13.70	13.60	13.65	170.43	13.02	13.04	13.03	170.99	170.71	52.53	134.2
5.14	5.14	5.14	178.94	4.70	4.68	4.69	179.33	179.135	55.12	140.1

Table 3(b). (Continued)

Creep deformation (10^{-3} inch units)									Creep strain (10^{-3} units)	Time in hours
Left				Right				Average of both sides		
(1)	(2)	Average	Total creep	(1)	(2)	Average	Total creep			
- 8.88	- 8.74	- 8.81	192.89	- 9.72	- 9.64	- 9.68	193.70	193.295	59.47	149.7
-19.76	-19.84	-19.80	203.88	-20.00	-20.04	-20.02	204.04	203.96	62.76	156.9
				44.62	44.36	44.49				
-32.26	-32.24	-32.25	216.33	31.28	31.32	31.30	217.23		66.56	165.0
33.14	33.14	33.14								
19.36	19.22	19.29	230.18	16.58	16.66	16.62	231.91		70.82	173.7
5.80	5.98	5.89	243.58	3.54	3.62	3.58	244.95		74.96	181.6
- 8.02	- 8.10	- 8.06	257.53	-10.72	-10.70	-10.71	259.24		79.24	189.8
				51.80	51.72	51.76				
-24.06	-24.22	-24.14	273.61	35.60	35.72	35.66	275.34		84.19	198.8
-35.90	-36.00	-35.95	285.42	22.22	22.28	22.25	288.75		87.82	205.8
32.78	32.94	32.86								
18.74	18.78	18.76	299.52	8.56	8.54	8.55	302.45		92.16	213.5
3.62	3.52	3.57	314.71	- 7.78	- 7.64	- 7.71	318.71		96.83	222.0
- 8.54	- 8.62	- 8.58	326.86						100.57	228.9
49.14	49.04	49.09								
36.00	35.88	35.94	340.01						104.62	236.0
18.16	18.26	18.21	357.74						110.07	245.6
0.40	0.46	0.43	375.52						115.54	254.6
-13.82	-13.84	-13.83	389.78						119.93	261.5
-20.90	-20.86	-20.88	396.73						122.07	271.1
43.56	43.58	43.57								

of such very low creep readings also contributes to the inconsistent readings. The readings are tabulated in Table 1.

The second test was conducted at 25,000 psi stress level. This test continued up to 1000 hours. In the author's opinion, the second test gave very good results. These are tabulated in Table 2.

The third test was at 35,000 psi stress level. The test went on smoothly up to 21.7 hours. The author could not measure creep after 27.8 hours as an unfortunate thing happened to the extensometer device approximately 24 hours after the test started. To make sure that there was no mistake in this conclusion, the author continued the test up to 58.6 hours. The results shown in Table 3(a) indicate that there was indeed a malfunction in the extensometer device. As a precautionary measure it was determined that the gearmotor functioned properly and that the furnace and its controller worked as usual. At this stage then, we suspected three reasons for this kind of failure. They were as follows:

(1) If two reference points are picked up on one of the platinum strips, there would not be any possibility of noticing creep on the extensometer device.

(2) At the end of the second test, when we tried to take out the extensometer brackets from the specimen, the spot welded joints at the two platinum strips of one bracket, marked X in Figure XV, separated and were only rewelded in an unsatisfactory manner. Also one of the stainless steel wires holding the platinum strip in position

with the bracket became rather short in length. It was suspected that these spot welded joints which were rewelded might have again become separated.

(3) One of the brackets of the extensometer device might have become loosened due to the stress relaxation of the allen screws at elevated temperatures.

It was decided that the first reason was highly improbable because the image of the object in the image plane was clear, the border line between the two platinum strips was clear, and the line marked on one platinum strip was discontinued at the border line.

The test was then terminated at 60 hours and inspected for the failure. The third reason listed above was found to be the correct one. Since the time available was very short, and there were no extra specimens on hand, we decided to continue the test on the same specimen. The extensometer device was again fitted to the same specimen with new allen screws and the test was again continued. The readings obtained are tabulated in Table 3(b). As mentioned in reason two above, one of the stainless steel wires holding the platinum strip in position with the bracket became shortened during rewelding process and the author could not measure the extension on this side after 222 hours. However, the readings tabulated for 156.9 hours in Table 3(b) showed the same creep readings taken from both sides of the extensometer device. Hence it was concluded that there would not be any appreciable error in the readings taken all from one side. Again the bracket was loosened after about 265 hours and there was no measurable creep after this incident. The test was continued so that the rupture time could be found at this stress and temperature, and it was found to be 569.1 hours (60 + 509.1).

Graphs

A family of creep-time curves can be obtained now from the data collected in those three tests. The creep strain and time measurements can be plotted to a linear scale on a graph paper as shown in Figure XVI. The minimum creep rate can be determined for each stress after establishing the minimum or constant creep rate period by approximating the points on the creep-time curve in the secondary creep to a straight line. The minimum creep rate vs. stress can be plotted on a log-log paper as shown in Figure XVIII. It will be a straight line for most of the stable metals and alloys.

Plotting the creep-time curves for the first two tests was quite satisfactory. Since the creep readings in the third test were unsatisfactory between 21.7 hours and 60 hours, special attention was needed in plotting the creep-time curve. To compensate for the creep that has occurred between 21.7 hours and 60 hours, the following technique was used. The creep-time curve up to 21.7 hours was plotted for the readings in Table 3(a) on one graph paper. The Table 3(b) readings belonged to the same specimen but actually started from and beyond 60 hours. So the graph of Table 3(b) slid on the graph of Table 3(a) by

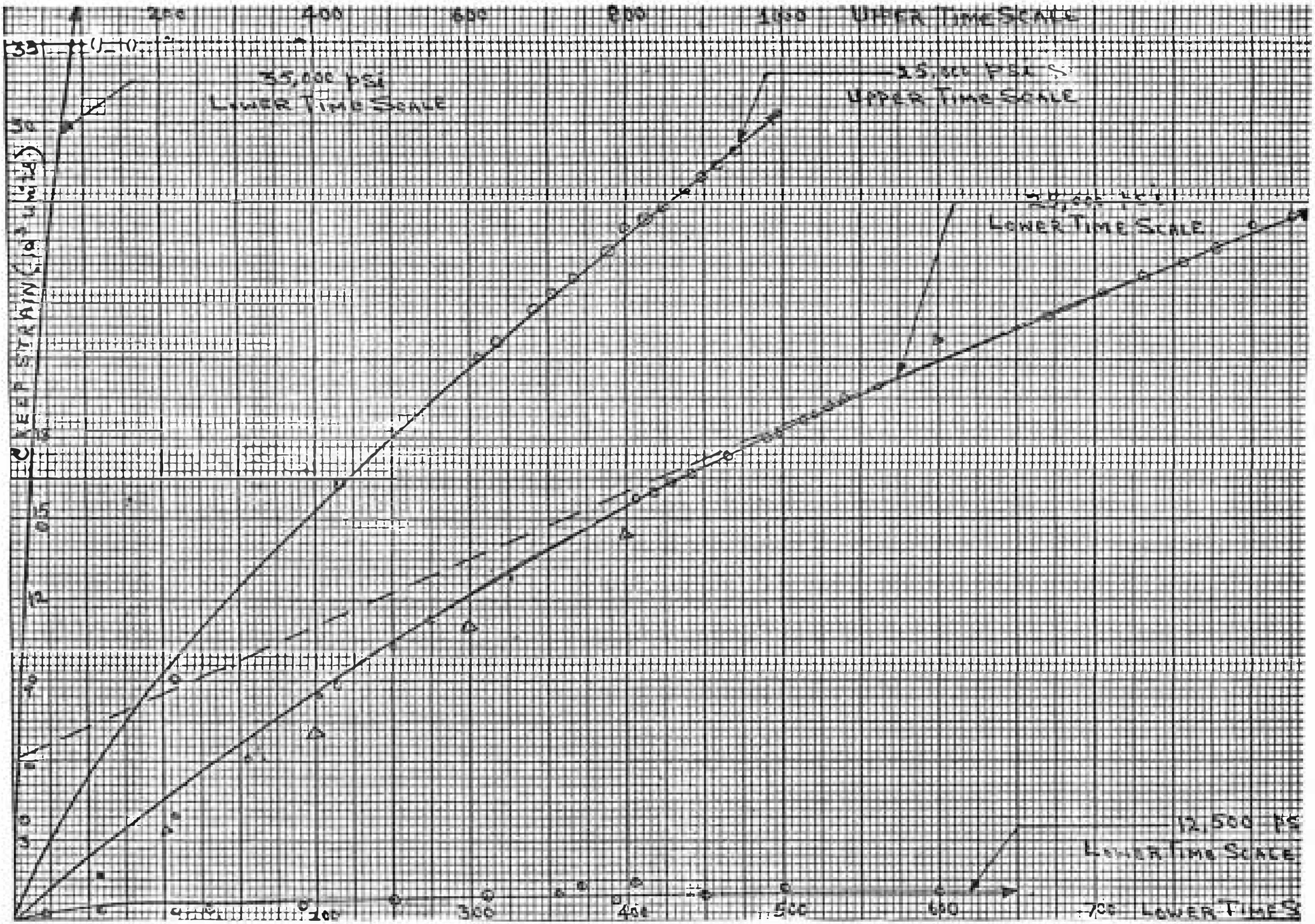

Figure XVI. Creep Time Curves for Hastelloy X Bar at 1200^{O}F.

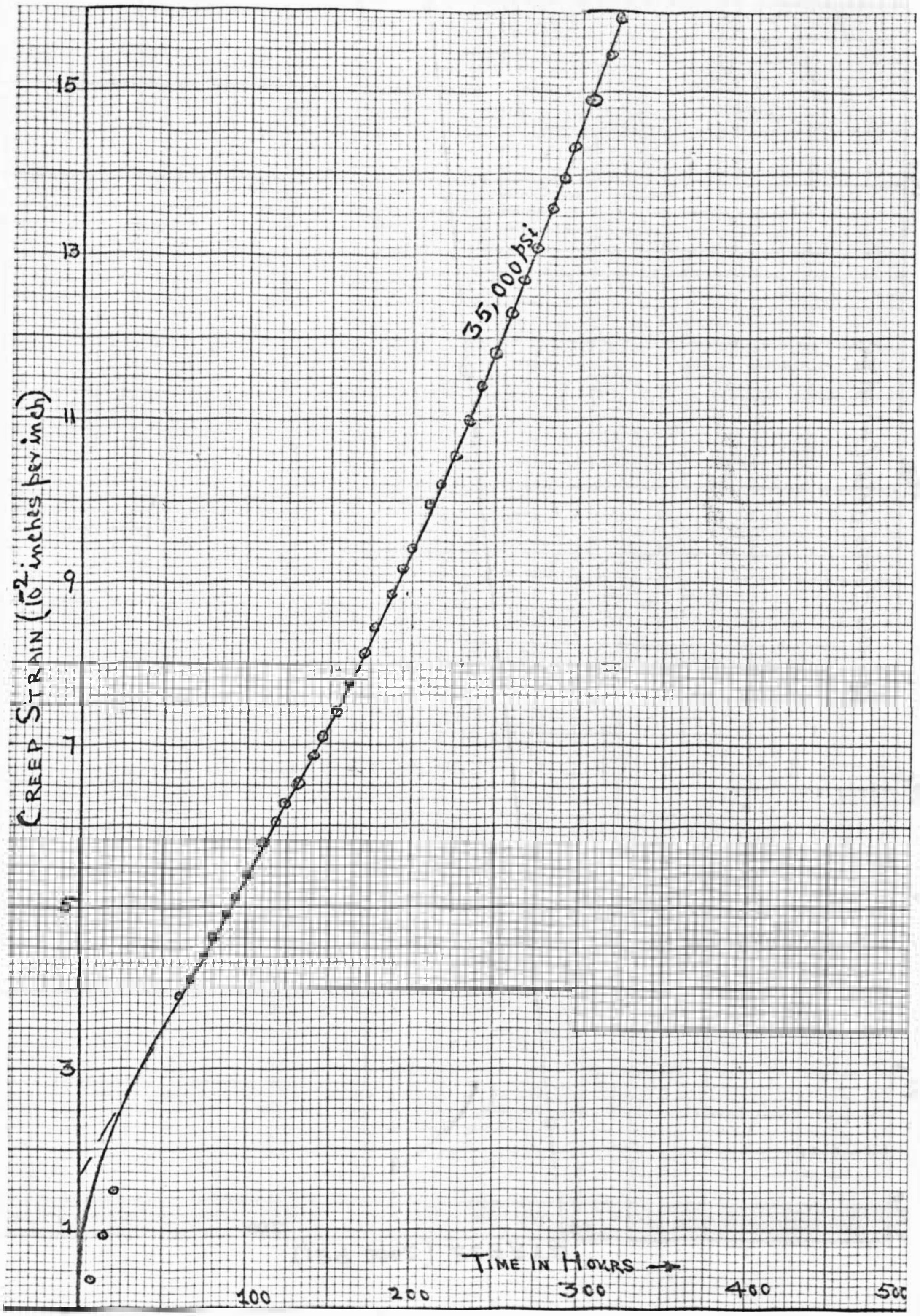

Figure XVII. Creep Time Curve for Hastelloy X at 1200°F.

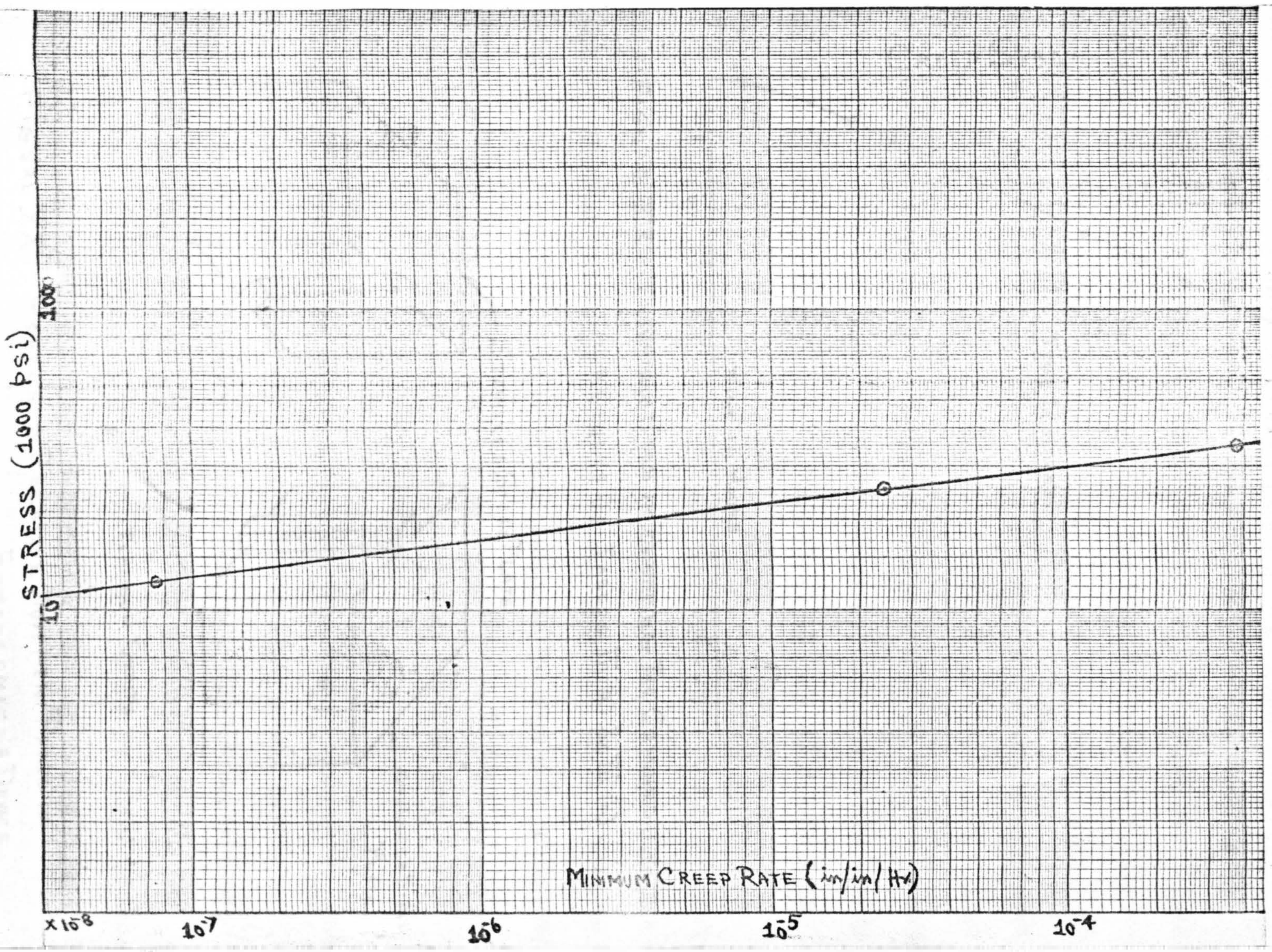

Figure XVIII. Minimum Creep Rate Vs. Stress at 1200°F. For Hastelloy X Bar

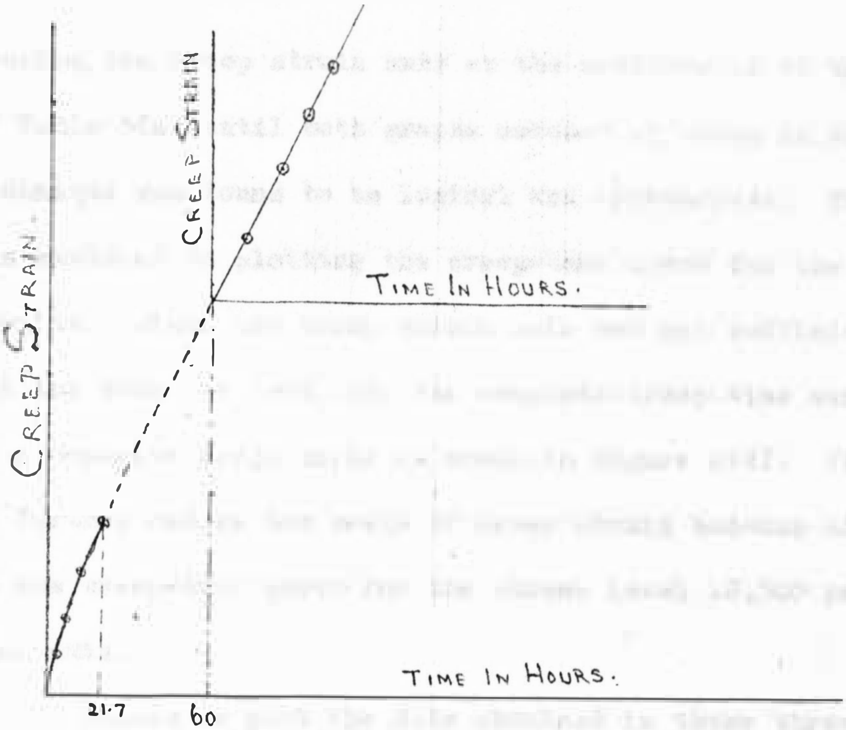

FIGURE XIX. TECHNIQUE USED IN PLOTTING THE COMINED RESULTS OF TABLES III (a) & III (b).

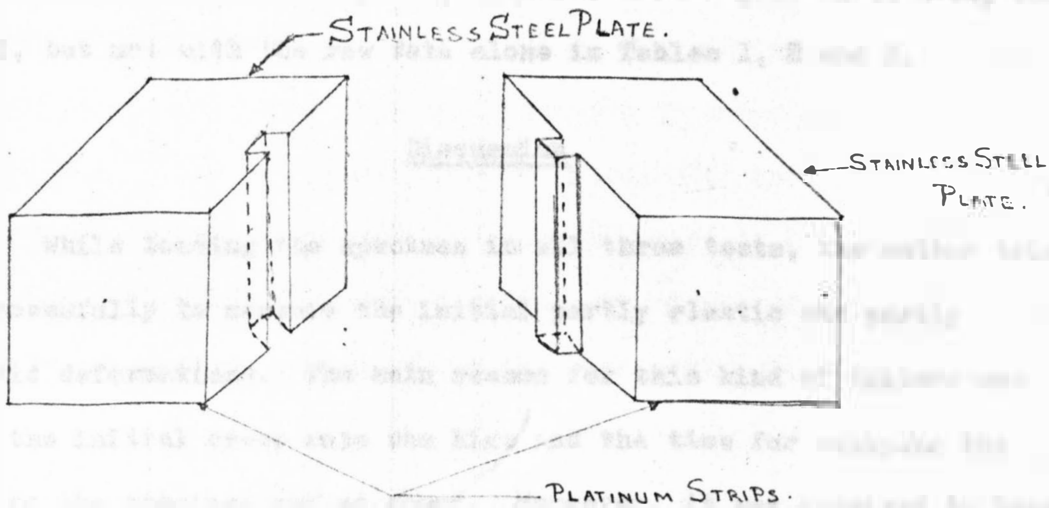

FIGURE XX. PROPOSED RELATIVE MOVEMENT PARTS IN EXTENSOMETER DEVICE.

keeping the creep strain axis at the ordinate of 60 hours of graph of Table 3(a) until both graphs matched as shown in Figure XIX. The technique was found to be logical and appropriate. This technique was employed in plotting the creep-time curve for the third test results. Since the creep strain axis was not sufficient to represent all the data for test III, the complete creep-time curve was plotted on a separate graph paper as shown in Figure XVII. It was not possible to further reduce the scale of creep strain because almost all points on the creep-time curve for the stress level 12,500 psi touched the time axis.

Unless we plot the data obtained in those three tests as shown in Figures XVI, XVII, and XVIII, we cannot make use of this data for design purposes. The interpolation or extrapolation of data will be possible only with the help of graphs shown in Figures XVI, XVII, and XVIII, but not with the raw data alone in Tables 1, 2 and 3.

Discussion

While loading the specimen in all three tests, the author tried unsuccessfully to measure the initial partly elastic and partly plastic deformations. The main reason for this kind of failure was that the initial creep rate was high and the time for applying the load to the specimen was so short. Moreover, it was required to take care of switching procedure for applying the load automatically.

The first test was not very satisfactory as explained under the item Results. In the author's opinion, the second test at 25,000 psi stress level gave very good results. However, it was clear from Figure XVI that the initial transient creep was very low. The reason may be in neglecting the initial plastic deformation on loading and immediately after loading (At very high stresses, this initial plastic deformation may be even 100 times the elastic deformation). Since there were no provisions to measure initial deformations with that kind of extension measuring apparatus, it was not appropriate to say the readings were not satisfactory.

Regarding minimum creep rate, the author could not find any published results to compare with the minimum creep rates that were obtained on Hastelloy alloy X bar material. It was found that the creep rate obtained in the second test of that material was the same as the published creep rate of a sheet of the same material. A comparison of minimum creep rate data provided by Union Carbide Corporation(13) on a Hastelloy alloy-X sheet with data on bar material published by Mathew J. Donachie, Jr., and Robert G. Shepheard(14) indicated that the minimum creep rates were higher with the sheet than with the bar material. From these two statements which are made in

---

(13) Union Carbide, "Hastelloy alloy-X," Union Carbide Corporation, Kokomo, Indiana, August 1961.

(14) Donachie, Mathew J., Jr., and Shepheard, Robert G., "Creep Rupture Behavior of Hastelloy X," A.S.T.M. Proceedings, Vol. 61, pp. 981, 1961.

this paragraph, it is apparent that the minimum creep rate obtained in the second test was higher than the actual minimum creep rate. The reason for obtaining this higher minimum creep rate may be due to the manner in which the author attached the extensometer device. The position of attachment is shown in Figure XV. The gauge length used for this set up was 3.25" as shown. It is possible to get a different minimum creep rate if the gauge length is taken as the center to center distance on the two brackets (distance B-B, on the sketch). If the standard gauge length is B-B as shown in the sketch, the effect of fillet radii and the increase in diameter due to the shoulders would probably complicate the problem. To adjust the error caused by this effect is theoretically impossible, but it is possible experimentally as explained in Recommendations and Conclusions.

Besides stresses and temperatures which will affect the minimum creep rates there are certain inherent characteristics of the metal and manufacturing variables including phase transformations, alloying elements, structure, grain size, precipitation effects, deoxidation practice, grain boundaries, etc. The other factors like cooling rate, crystal growth, heat treatment process, dislocations present in the crystal and manufacturing variables like the furnace used for melting, casting, extruding, rolling, etc., also affect the minimum creep rate. There will be a lot of difference in minimum creep rate between a cold rolling material and a hot rolling material even though the chemical composition is the same. The effect of hot working is the grain refinement brought about by recrystallization. The coarse structure is definitely broken up and elongated by the rolling action. Because of the high temperature, recrystallization starts immediately and small grains start to form and grow rapidly until the recrystallization is complete. Creep resistance is also influenced by the grain size of the material; at temperatures below the lowest temperature of recrystallization, a fine grained steel possesses the greater resistance, whereas at temperatures above that point, a coarse grained steel is more creep resistant. Another important probable factor influencing creep is presence of more dislocations in a cold worked material. The more dislocations there are, the more the slip takes place in a crystal. Regarding heat treatment process, the bar is solution heat treated (2250°F and water quenched), whereas the sheet is solution heat treated, 2150°F and rapid air cooled.

Some of these factors contribute to higher creep rates in a sheet material than in a bar even though the chemical composition is the same.

EXTRAPOLATION OF DATA

From a family of creep-time curves, the Engineer must devise methods of extrapolating the data for longer periods of time depending on the life of the machine element subjected to high temperatures. Because of obsolescence and because of the heavy financial burden it is not desirable to conduct tests in order to determine the total creep that may occur during the entire lifetime of the part. In any case, the extrapolation of data is essential for all applications of creep data, i.e., in any design of machine element with a longer useful lifetime at elevated temperatures.

Extrapolation of the rate of secondary creep has been employed to provide design data for engineering applications. For this purpose the creep test must continue long enough to define the slope of the creep-time curve in the constant rate or third stage. In the design of the machine member subjected to high temperature, it is assumed that the material will not pass into the tertiary stage during the useful lifetime. Several methods are available to extrapolate the data. The constant creep rate lines in Figures XVI and XVII can be extrapolated without much appreciable error. The graph plotted on a log-log paper between minimum creep rate and stress will be a straight line for most of the stable metals. Similarly the graph plotted between the stress on a linear scale and minimum creep rate on a logarthmic scale will be a straight line. Usually it is possible to extrapolate the data with assurance if there is a linear relation between any two variables.

Fitting a Creep-Time Curve

It is not an easy task to fit all the experimental data with a simple expression. First the author tried to fit the experimental data obtained in the creep test with a logarthmic curve. No one can exactly fit all those 68 observations in the second test by a mathematical model. What we have to find is some compromise curve which will come as near as possible agreeing with all the 68 observations in the second test. There are three equations that can fit well enough these logarthmic curves. These are of the form:

$$\text{Log(Creep strain)} = a + b\ \text{(time)} \qquad (1)$$

$$\text{Creep strain} = a + b\ \text{Log(time)} \qquad (2)$$

$$\text{Log(Creep strain)} = a + b\ \text{Log(time)} \qquad (3)$$

where a and b are experimental constants which depend on stress and temperature at which the test is conducted.

Equation (3) fits the author's experimental data better than the other two equations. This conclusion has been reached when the observations are plotted log(creep strain) versus time, creep strain versus log(time), and log(creep strain) versus log(time) on a graph paper. It is found log(creep strain) versus log(time) is a better approximation to a straight line than the other two cases. The constants a and b are evaluated by using the principle of the method of least squares. The expressions used in finding the constants a and b are developed in Appendix B. The constants a and b calculated in this way for 25,000 psi stress level are as follows:

$$a = -4.53116, \qquad b = 1.0343$$

Hence equation (3) will be

$$\log(\text{creep strain}) = -4.53116 + 1.0343 \log(\text{time})$$

This expression did not fit well for the 25,000 psi stress level experimental data. The points obtained with the help of this expression are enclosed by small triangles in Figure XVI.

Since this expression is not valid, we shall now apply the principle of least squares to the fitting of experimental data by polynomials. There are 68 observations, and let it be desired to fit these readings with a second degree polynomials.

That is of the form

$$= a_o + a_1 t + a_2 t^2$$

where

t = time in hours.

a_o, a_1, a_2 are constants.

The procedure used to calculate the constants a_o, a_1, and a_2 is explained in Appendix C. The numerical calculations are shown below.

The summations that are required to form normal equations are tabulated in Table 4.

$$F_1 = 68 + 28859.7 + 16659161 + 1.026237 = 16688089$$

$$F_2 = 28859.7 + 16659161 + 1.1063335 \times 10^{10} + 573.8846 = 1.1080024 \times 10^{10}$$

Table 4. Quantities Required to Fit the Data of 25,000 Psi Stress Level With an Equation, $\epsilon_t = a_o + a_1 t + a_2 t^2$

t^o	t	t^2	$t^3 (x10^5)$	$t^4 (x10^8)$	$\epsilon (x10^{-3})$	$t\epsilon (x10^{-2})$	$t^2\epsilon$
1	10.6	112.36	0.01191016	0.00012625	0.288	0.3053	0.032360
1	23.0	529.00	0.12167000	0.00279841	0.491	1.1293	0.259739
1	34.9	1218.01	0.42508549	0.01483524	0.863	3.0119	1.051134
1	45.7	2088.49	0.95443993	0.04361790	1.180	5.3926	2.464418
1	57.2	3271.84	1.8714925	0.10704937	1.697	9.7068	5.552312
1	71.7	5140.89	3.6860181	0.26428750	2.321	16.6416	11.932006
1	83.8	7022.44	5.8848047	0.49314664	2.758	23.1120	19.367889
1	94.3	8892.49	8.3856181	0.79076378	3.389	31.9583	30.136649
1	107.6	11577.76	12.457670	1.3404453	4.06	43.6856	47.005706
1	118.8	14113.44	16.766767	1.9918919	4.58	54.4104	64.639555
1	130.4	17004.16	22.173425	2.8914146	5.15	67.1560	87.571424
1	142.7	20363.29	29.058415	4.1466358	5.70	81.3390	116.07075
1	154.7	23932.09	37.022943	5.7274493	6.18	95.6046	147.90032
1	166.6	27755.56	46.240763	7.7037111	6.75	112.4550	187.35003
1	178.8	31696.44	57.161359	10.220451	7.37	131.7756	235.61477
1	190.7	36366.49	69.350896	13.225216	7.97	151.9879	289.84092
1	203.0	41209.00	83.654270	16.981817	8.48	172.1440	349.45232
1	215.0	46225.00	99.383750	21.367506	8.92	192.8550	414.63825
1	226.8	51438.24	116.66193	26.458925	9.42	213.6456	484.54822
1	238.8	57025.44	136.17675	32.519008	9.90	236.4120	564.55186
1	251.3	63151.69	158.70020	39.881359	10.33	259.5929	652.35696
1	263.2	69274.24	182.32980	47.989203	10.73	282.4136	743.31260
1	275.0	75625.00	207.96875	57.191406	11.33	311.5750	856.83125
1	287.2	82483.84	236.89359	68.035839	11.81	339.1832	974.13415
1	298.8	89281.44	266.77294	79.711755	12.17	363.6396	1086.5551
1	310.9	96658.81	300.51224	93.429256	12.63	392.6667	1220.8008
1	321.4	103297.96	331.99964	106.70468	12.91	414.9274	1333.5767

Table 4. (Continued)

t^0	t	t^2	$t^3(x10^5)$	$t^4(x10^8)$	$\epsilon(x10^{-3})$	$t\epsilon(x10^{-2})$	$t^2\epsilon$
1	334.8	112091.04	375.28080	125.64401	13.45	450.3060	1507.6245
1	346.0	119716.00	414.21736	143.31921	13.84	478.8640	1656.8694
1	358.7	128665.69	461.52383	165.54860	14.29	512.5823	1838.6327
1	370.7	137418.49	509.41034	188.83841	14.69	544.5583	2018.6776
1	381.8	145771.24	556.55459	212.49254	14.99	572.3182	2185.1109
1	394.8	155867.04	615.36307	242.94534	15.40	607.9920	2400.3524
1	407.0	165649.00	674.19143	274.39591	15.74	640.6180	2607.3153
1	419.0	175561.00	735.60059	308.21665	16.08	673.6520	2823.0209
1	430.0	184900.00	795.07000	341.88010	16.43	706.4900	3037.9070
1	442.6	195894.76	867.03021	383.74756	16.80	743.5680	3291.0320
1	454.5	206570.25	938.86179	426.71268	17.17	780.3765	3546.8120
1	466.0	217156.00	1011.9470	471.56728	17.48	814.5680	3795.8869
1	478.9	229345.81	1098.3342	525.99225	17.82	853.3998	4086.9316
1	491.1	241179.21	1184.4311	581.67411	18.15	891.3465	4377.4027
1	502.6	252606.76	1269.6016	638.10175	18.45	927.2970	4660.5947
1	514.9	265122.01	1365.1132	702.89680	18.77	966.4673	4976.3401
1	526.6	277307.56	1460.3016	768.99683	19.10	1005.8060	5296.5744
1	539.2	290736.64	1567.6520	845.27794	19.42	1047.1264	5646.1055
1	551.0	303601.00	1672.8415	921.73567	19.69	1084.9190	5977.9037
1	562.9	316856.41	1783.5847	1003.9798	20.07	1129.7403	6359.3081
1	574.4	329935.36	1895.1487	1088.5734	20.39	1171.2016	6727.3820
1	587.4	345038.76	2026.7577	1190.5175	20.74	1218.2676	7156.1039
1	597.5	357006.25	2133.1123	1274.5346	20.97	1252.9575	7486.4211
1	611.1	373443.21	2282.1115	1394.5983	21.35	1304.6985	7973.0125
1	621.7	386510.89	2402.9382	1493.9067	21.64	1345.3588	8364.0957
1	634.0	401956.00	2548.4010	1615.6863	21.88	1387.1920	8794.7973
1	646.7	418220.89	2704.6345	1749.0871	22.25	1438.9075	9305.4148
1	659.0	434281.00	2861.9118	1885.9999	22.55	1480.0450	9793.0365
1	671.0	450241.00	3021.1171	2027.1696	22.83	1531.8930	10279.002

Table 4. (Continued)

t^0	t	t^2	$t^3 (x10^5)$	$t^4 (x10^8)$	$\epsilon (x10^{-3})$	$t\epsilon (x10^{-2})$	$t^2\epsilon$
1	684.2	468129.64	3202.9430	2191.4536	23.16	1584.6072	10841.882
1	706.9	499707.61	3532.4331	2497.0770	23.72	1676.7668	11853.064
1	732.7	536849.29	3933.4947	2882.0716	24.30	1780.4610	13045.438
1	756.0	571536.00	4320.8122	3266.5340	24.84	1877.9040	14196.954
1	778.4	605906.56	4716.3767	3671.2276	25.36	1974.0224	15365.790
1	802.8	644487.84	5173.9484	4153.6458	25.92	2080.8576	16705.125
1	827.0	683929.00	5656.0928	4677.5888	26.51	2192.3770	18130.958
1	850.5	723350.25	6152.0939	5232.3558	27.02	2298.0510	19544.924
1	875.1	765800.01	6701.5159	5864.4966	27.57	2412.6507	21113.106
1	898.5	807302.25	7253.6107	6517.3692	28.18	2531.9730	22749.777
1	922.6	851190.76	7853.0860	7245.2571	28.64	2642.3264	24378.103
1	946.2	895294.44	8471.2760	8015.5213	29.16	2759.1192	26106.786
68	28859.7	16659161	1.1063335	7.9847868	1.026237	573.8846	371929.12
$= S_0$	$= S_1$	$= S_2$	$x 10^{10} = S_3$	$x 10^{12} = S_4$	$= K_0$	$= K_1$	$= K_2$

$F_3 = 16659161 + 1.1063335 \times 10^{10} + 7.9847868 \times 10^{12}$

$+ 371929 = 799.58671 \times 10^{10}$

$A_1 = 68$

$A_2 = 28859.7$

$A_3 = 16659161$

$B_1 = \frac{28859.7}{68} = 424.40735$

$C_1 = \frac{16659161}{68} = 244987.66$

$D_1 = \frac{1.026237}{68} = 0.01509172$

$E_1 = \frac{16688089}{68} = 245413.07$

Check: $1 + B_1 + C_1 + D_1 = 245413.07 = E_1$

$B_2 = 16659161 - 424.40735 \times 28859.7 = 4410892$

$B_3 = 1.1063335 \times 10^{10} - 424.40735 \times 16659161 = 3.9930646$

$\times 10^9$

$C_2 = \frac{1.1063335 \times 10^{10} - 244987.66 \times 28859.7}{4410892} = 905.27383$

$D_2 = \frac{573.8846 - 0.01509172 \times 28859.7}{4.410892 \times 10^6} = 3.1363747 \times 10^{-5}$

$E_2 = \frac{1.1080024 \times 10^{10} - 245413.07 \times 28859.7}{4.410892 \times 10^6} = 906.27392$

Check: $1 + C_2 + D_2 = 906.27386 = E_2$

$C_3 = 7.9847868 \times 10^{12} - 905.27383 \times 3.9930646 \times 10^9$

$- 244987.66 \times 16659161 = 288.681 \times 10^9$

$$D_3 = \frac{371929.12-3.1363747\times10^{-5}\times3.9930646\times10^{9}-0.01509172\times16659161}{288.681\times10^{9}}$$

$$E_3 = \frac{799.58671\times10^{10}-906.27392\times3.9930646\times10^{9}-245413.07\times16659161}{288.681\times10^{9}} = 1$$

Solutions:

$$a_2 = -1.6363183\times10^{-8}$$

$$a_1 = 3.1363747\times10^{-5} - 905.27383\times(-1.6363183\times10^{-8})$$

$$= 4.6176908\times10^{-5}$$

$$a_o = 0.01509172 - 244987.66\times(-1.6363183\times10^{-8})$$

$$-424.40735\times4.6176908\times10^{-5} = -4.97321\times10^{-4}$$

$$\in = -4.97321\times10^{-4} + 4.6176908\times10^{-5}\,t - 1.6363183\times10^{-8}\,t^2$$

This expression fitted very well for the entire test period, i.e., 1000 hours. The creep strain increases with time up to 1411 hours and from there decreases due to the second degree negative term increasing more rapidly than the first degree positive term. This maximum point can be found by differentiating with respect to t.

$$\text{i.e., } \frac{d\in}{dt} = a_1 + 2a_2 t = 0$$

$$t = \frac{-a_1}{2a_2} = \frac{4.61769\times10^{-5}}{3.27264\times10^{-8}} = 1411 \text{ hours}$$

The expression to find the total creep beyond the test period up to anywhere in the secondary creep region can be written similar to the following form.

$$\epsilon = \epsilon_{t_1} + C(t - t_1)$$

where t_1 is less than 1000 hours (the test period),

ϵ = Creep strain at a time t

C = Minimum creep rate

Example:

For the test 1200°F, 25,000 psi stress level, the total creep strain at 2500 hours would be

$$\epsilon_{2500} = \epsilon_{800} + 2.4353 \times 10^{-5} (2500-800)$$

But from the above second degree polynomial expression,

$$\epsilon_{800} = - 4.97321 \times 10^{-4} + 4.6176908 \times 10^{-5}(800)$$

$$- 1.6363183 \times 10^{-8}(800)^2$$

$$= 2.59725264 \times 10^{-2}$$

$$\epsilon_{2500} = 2.59725 \times 10^{-2} + 2.4353 \times 10^{-5}(2500-800)$$

$$= 6.73726 \times 10^{-2}$$

Minimum Creep Rate - Stress Relationship

The minimum creep rate for any other stress not covered in the above tests can be obtained from the graph shown in Figure XVIII. Since this graph is a straight line, it is also possible to establish a relation between the minimum creep rate and the stress at the test temperature.

The general expression for such a straight line would be

$$C = a\,S^b$$

where C = minimum creep rate in inches per inch per hour

S = stress in psi

a and b are constants.

The same expression can also be written as

$$\log C = \log a + b \log S$$

where $\log a$ = intercept on the minimum creep rate axis

and b = slope of the straight line

= 8.2353 (obtained from the graph in Figure XVIII)

Since the straight line is not intersecting the minimum creep rate axis within the graph paper, the intercept can be found by solving any one linear relation correspond to that straight line graph. This can be done as follows:

$$\log(2.4353 \times 10^{-5}) = \log a + 8.2353 \log(25{,}000)$$

or $\log a = -40.8792 = \overline{41}.1208$

Hence, $a = 1.3206 \times 10^{-41}$

Therefore, minimum creep rate - stress relationship is

$$\underline{C = 1.3206 \times 10^{-41} S^{8.2353}}$$

When there are many points which are spread considerably and when it is not possible to join them in one straight line, the method of least squares is the best fit for such a situation and the constants in the expression can be evaluated as follows:

The minimum creep rates obtained on Hastelloy alloy-X bar material at 1200°F and at 12,500 psi and 35,000 psi stress levels are 0.75×10^{-7}, 2.4353×10^{-5} and 3.7742×10^{-4} in/in/hr. respectively.

Relationship between the two variables is $C = a(S)^b$ or

$\log. C = \log. a + b \log. S$ or $\bar{C} = \log. a + b\,\bar{S}$

The required quantities to substitute in equations (5) and (6) are summarized in Table 5.

Table 5. Quantities to Evaluate the Constants in the Relation Between Minimum Creep Rate and Stress

$\bar{C}$	$\bar{S}$	$\overline{CS}$	$(\bar{S})^2$
$\bar{8}.8751 = -7.1249$	4.0969	- 29.19	16.7746
$\bar{5}.3865 = -4.6135$	4.3979	- 20.2897	19.3415
$\bar{4}.5768 = -3.4232$	4.5441	- 15.5554	20.6488
-15.1616	13.0389	- 65.0351	56.7649

$$A_{\bar{C}} = \frac{\Sigma \bar{C}}{n} = -\frac{15.1616}{3} = -5.0539$$

$$A_{\bar{S}} = \frac{\Sigma \bar{S}}{n} = \frac{13.0389}{3} = 4.3463$$

$$b = \frac{\Sigma\,\overline{SC} - nA_{\bar{C}}\,A_{\bar{S}}}{\Sigma(\bar{S})^2 - n(A_{\bar{S}})^2} = \frac{-65.0351 + 3 \times 5.0539 \times 4.3463}{56.7649 - 3(4.3463)^2} = 8.1416$$

$$\log. a = A_{\bar{C}} - n\,(A_{\bar{S}})$$

$$= -5.0539 - 3(4.3463)$$

$$= -40.4397$$

$$= \overline{41}.5603$$

$$a = 3.633 \times 10^{-41}$$

Hence, minimum creep rate - stress relationship is

$$C = 3.633 \times 10^{-41} (S)^{8.1416}$$

This relationship can be used to find stress distribution in a design problem when there is both combined bending and direct load, and steady creep. The relationship can also be used to predict the minimum creep rate for any other stress at the test temperature 1200°F.

APPLYING THE DATA IN A DESIGN PROBLEM

The amount that a member deforms or creeps depends upon the stress, temperature, machining, pre-history of the material in casting, heat treatment and the chemical composition of the material. Moreover, the materials which will have the same characteristics at room temperature may differ in creep characteristics at higher temperatures. So, suitable values for working stresses at high temperatures can be determined only by experimental methods.

When the part operates at high temperatures with a close clearance, the designer must predict the amount of creep that may take place during the entire life of the member. Where these close clearances are not involved, the permissible creep deformations are limited by taking into account the total deformations that may cause the embrittlement and fracture. In either case, the creep data is essential.

Sometimes designs may impart brittleness tendencies to materials which would otherwise be ductile. If a bar is subjected to an uniaxial load, necking takes place as it approaches fracture. If the same bar is loaded laterally as well as axially and if these lateral loads are high enough, plastic behavior can be suppressed to the point where the bar would break in a brittle manner with no elongation and no reduction in area. So the complete analysis of the various forces which will act on a member to be designed is very important.

Sometimes the concepts of a limiting creep stress can be used in a design problem. H. J. Tapsell[15] defines the limiting creep stress as "the load per unit of the original area which will just not break the bar when allowed to remain for a long time." This limiting creep stress with a proper factor of safety may be used as the safe working stress in design using the formulas based on elastic theory. The part designed in this way may deform with time even though it would not break. So this procedure may not be very satisfactory.

The experiments on creep show that the creep rate is particularly sensitive to temperature changes. Even if there is 25°F higher than designed temperature, it may amount to an increase in the creep rate of 6 to 10 times, depending on the temperature at which it is to be operated. So sufficient allowance must be made for possible temperature fluctuations and the design must be based on the maximum temperature rather than on an average temperature.

The designer must also bear in mind that extrapolating on 1000 hour tests and using in design is a matter of chance. So the designer must be careful in selecting suitable methods for extrapolating the data and in using proper safety factors to compensate for the unknown variables.

Since the mechanical reliability and useful service life of a gas turbine plant are governed almost entirely by the design of power

---

[15] Tapsell, H. J., "Creep of Metals," Oxford University Press, London, 1931.

element, such a design must be based on high efficiency, dependability and low first cost. The most important factors to be considered before designing any gas turbine power element are expected useful service life, maximum steady load and variable load and the desired efficiency. According to H. D. Emmert,(16) these principles contribute to adopting mulfiple stages, employing maximum blade height ratios in the low pressure elements and rotating at a maximum speed.

Here in this brief discussion, the author's object is to consider the creep aspect of view only, i.e., analyzing the forces acting on a turbine blade, and to apply the experimental creep data and its results in the design of this turbine blade. The author has to assume certain data as known, especially the fluid mechanics and the mechanical design of the turbine blade path.

Creep rate and total deformation data can be used for establishing actual working stresses for rotating parts. Fatigue strength at operating temperature is of considerable importance in selecting blade materials. Accurate fatigue data are not available for many high temperature alloys. Hence compensation must be provided by limiting bending stresses as much as possible, and by controlling blade vibrational characteristics.

---

(16)Emmert, H. D., "Current Design Practices for Gas Turbine Power Elements," Trans. A.S.M.E., Vol. 72, pp. 189, February 1950.

The following important factors should be considered in selecting the permissible working stresses. The machine must be protected against failure due to either fracture or excessive deformations that may occur due to the extra peak load conditions. According to Weaver,[17] stability of steels should also be taken into account and protection should be provided against any changes in structure after it is installed. Some allowance also must be provided due to inaccuracies in stress analysis in complicated machine elements.

Analyzing the Stresses Acting on a Turbine Blade

The forces acting on a turbine blade are centrifugal and bending forces generated by rotation and fluid pressure differences respectively. The highest stresses acting on the turbine blades are due to centrifugal forces in the rotating parts and these stresses will act at the root of a blade. This can be calculated by using the following equation:

$$S_c = 4.52 \quad f_t \; A \; (N/1000)^2$$

Where f_t = taper factor, can be obtained from a graph

= specific weight of the material in pounds per cubic inch

N = speed in R.P.M.

A = annular flow area in square inches

S_c = average tensile stress due to centrifugal forces in psi

---

[17] Weaver, op. cit., pp. 745-751.

The derivation of this equation can be obtained from any standard textbook on gas turbines. The principle employed in deriving this equation is Newton's second law of motion. Consider an elemental mass. The centrifugal force acting on this elemental mass is the product of mass and acceleration. The equation mentioned on the preceeding page can be obtained by integrating this to the entire mass.

The bending stresses are produced in a turbine blade by the forces resulting from fluid velocity changes (F_x) and pressure differences across the blade row (F_y). The expressions for the bending moments produced due to these two forces can be obtained from "Theory and Design of Steam and Gas Turbines" by John F. Lee[18] or from any other standard textbook on gas turbines. The expressions are as follows:

Bending moment around the X-axis of the root section = M_x

$$= \frac{\pi \, r_m \, V_x \, h^2 \, \Delta V_m}{g \, v \, z} \text{ lb. ft.}$$

Where

r_m = mean radius of blade row in feet

V_x = axial velocity of air in ft./sec.

h = blade length in ft.

ΔV_m = change in rotational velocity component of air at mean radius in ft./sec.

g = gravitational constant in ft./sec.^{2}

---

(18) Lee, John F., "Theory and Design of Steam and Gas Turbines," McGraw Hill Book Company, Inc., New York, 1954.

v = specific volume of air in cu. ft./lb.

z = number of blades

Here assumed that it is having a free vortex stage.

Bending moment around the y-axis and the root section = My

$$= \frac{\pi h^2 \quad \Delta P \, (2 \, r_t + r_r)}{3z} \text{ lb. ft.}$$

Where ΔP = change in pressure across the blade row in lb./sq. ft.

r_t = radius of the turbine wheel to the tip of the blade row in feet

r_r = radius to the root of the blade row in feet

The next step is transferring these moments to the principal axes P and Q. The properties of a principal axis are the following.

(1) The moment of inertia at the intersecting point of the principal axes is either greater or lesser than at any other axis passing through that point.

(2) The product of inertia for these principal axes is zero.

These principal axes can be found by using the relation given by Seely[19] as

$$\tan 2\theta = \frac{2 \, I_{xy}}{I_y - I_x}$$

Where θ = angle between the principle axis and X-axis (shown in Figure XXI)

I_{xy} = product of inertia about x and y axes

I_x and I_y are moments of inertia about x and y axes respectively.

---

[19] Seely, Fred B., Ensign, Newton E., and Jones, Paul G., "Analytical Mechanics for Engineers," John Wiley & Sons, Inc., New York, 1958.

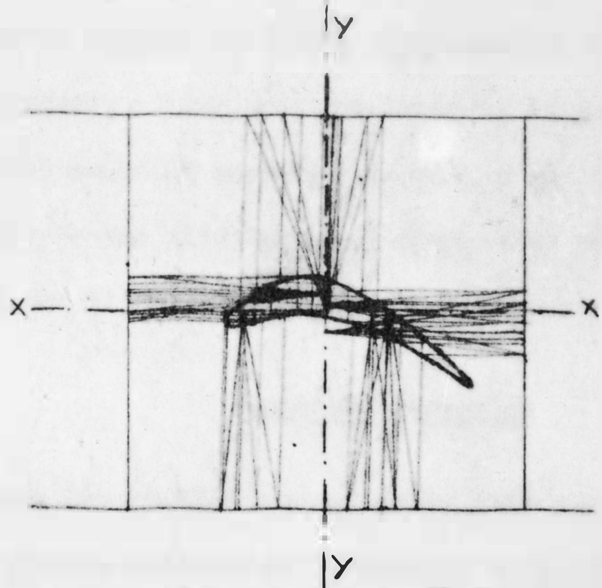

(a) GRAPHICAL CONSTRUCTION TO FIND MOMENT OF INNERTIA.

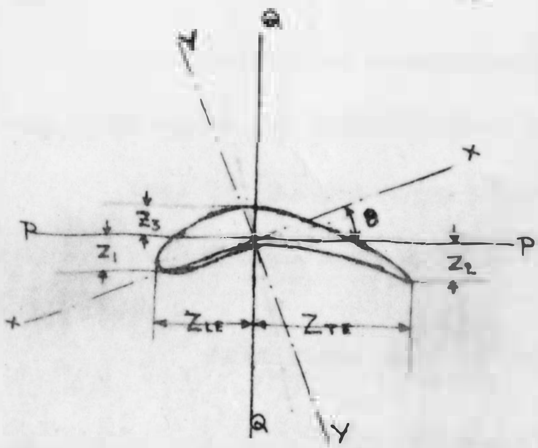

(b) PRINCIPAL AXES & SECTION MODULI.

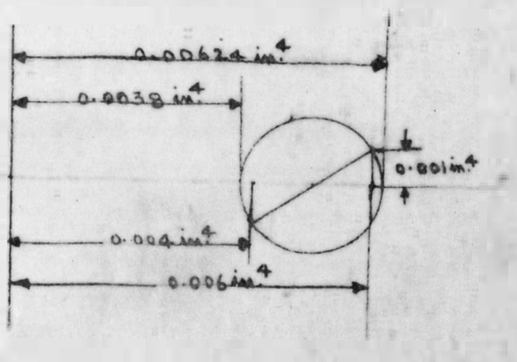

(C) MOHR'S CIRCLE.

FIGURE XXI. DESIGN OF REACTION TURBINE BLADE.

Accurate control of blade frequency is required to limit the vibrating stresses within the data assumed in stress analysis. The design must be suitably modified in such a way that the frequency corresponding to the first mode of transverse vibration lies above the fourth multiple of the maximum rotational speed.

Numerical Example

To show the application of creep data in design, the author has taken one standard profile of a reaction turbine blade shown in Figure XXI and also assumed the following data to complete the problem.

Temperature of gas flow is 1200°F. Assumed the blade under design is in free vortex stage, $r_r = 7''$, $r_t = 13''$, N = 6000 R.P.M., z = 80, $\Delta P = 10$ psi, $V_x = 260$ ft./sec., P = 50 psi, $V_m = 380$ ft./sec., specific weight of the Hastelloy alloy X bar material is 0.297 lb./cu. in.

The area of the reaction blade root profile in Figure XXI is measured with a planimeter and found to be as 0.17 sq. in.

Area of the reaction blade tip profile = 0.085 sq. in.

$$h = r_t - r_r = 13 - 7 = 6''$$

$$\text{Area ratio} = \frac{0.085}{0.17} = 0.5$$

$$h/\,2r_m = \frac{6}{2\left(\frac{7+13}{2}\right)} = 0.3$$

Assuming the taper as between linear and conical taper, the taper factor from the graph by Emmert[22] can be found by interpolation and is equal to 0.725.

$$v = \frac{RT}{P} = \frac{53.3\ (1200 + 460)}{50 \times 144} = 12.25 \text{ cu.ft./lb.}$$

$$A = \pi (r_t^2 - r_r^2) = \pi (13^2 - 7^2) = 376.8 \text{ sq.in.}$$

$$S_c = 4.52\ \gamma\ f_t\ A(N/1000)^2$$

$$= 4.52 \times 0.297 \times 0.3 \times 376.8 \times (6000/1000)^2$$

$$= 13{,}266 \text{ psi}$$

$$M_y = \frac{\Delta p\ \pi\ h^2}{3\ z} (2r_t + r_r)$$

$$= \frac{10\ \pi\ (6)^2}{3 \times 80} \left(\frac{2 \times 13 + 7}{12}\right)$$

$$= 13 \text{ lb.in.}$$

$$M_x = \frac{\pi\ r_m\ V_x\ h^2\ \Delta V_m}{g\ v\ z}$$

$$= \frac{\pi \times 10/12 \times 260 \times (6/12)^2 \times 380}{32.2 \times 12.25 \times 80}$$

$$= 2.05 \text{ lb.ft.} = 24.6 \text{ lb.in.}$$

At this stage, a graphical construction is used to find the moments of inertia I_x and I_y as shown in Figure XXII (a) and obtained the following results.

$$I_x = 0.006 \text{ in}^4,\quad I_y = 0.004 \text{ in}^4,\quad I_{xy} = 0.001 \text{ in}^4$$

---

[22] Emmert, op. cit., pp. 197.

The direction of principal axis can be found as follows.

$$\text{Tan } 2\theta = \frac{2\, I_{xy}}{I_y - I_x} = \frac{2 \times 0.001}{0.006 - 0.004} = 1$$

$$\theta = 22.5 \text{ degrees or } 112.5 \text{ degrees}$$

The Mohr's circle can be constructed to get the moment of inertia about the principal axis and it is shown in Figure XXI (c)

$$I_p = 0.00624 \text{ in}^4, \quad I_q = 0.0038 \text{ in}^4$$

Section Module:

$$Z_1 = I_p / z_1 = 0.00624/0.17 = 0.0367 \text{ in}^3$$

$$Z_2 = I_p / z_2 = 0.00624/0.2 = 0.0312 \text{ in}^3$$

$$Z_3 = I_p / z_3 = 0.00624/0.155 = 0.0403 \text{ in}^3$$

$$Z_{LE} = I_q / z_{LE} = 0.0038/0.5 = 0.0076 \text{ in}^3$$

$$Z_{TE} = I_q / z_{TE} = 0.0038/0.8 = 0.00475 \text{ in}^3$$

Bending moments about the principal axes P and Q:

$$M_p = M_y \sin\theta + M_x \cos\theta$$

$$= 13 \sin 22.5 + 24.6 \cos 22.5$$

$$= 27.5 \text{ lb.in.}$$

$$M_q = M_y \cos\theta - M_x \sin\theta$$

$$= 13 \cos 22.5 - 24.6 \sin 22.5$$

$$= 2.5 \text{ lb. in.}$$

Bending Stresses:

$$S_{LE} = M_p/Z_1 + M_q/Z_{LE} = 27.5/0.0367 + 2.5/0.0076 = 1079 \text{ psi}$$

$$S_{TE} = M_p/Z_2 - M_q/Z_{TE} = 27.5/0.0312 - 2.5/0.00475 = 354 \text{ psi}$$

$$S_B = - M_q/Z_3 = - 2.5/0.0403 = - 62 \text{ psi}$$

Minus sign indicates compression.

Maximum steady stress at the concave side of the leading edge = $S_c + S_{LE} = 13{,}266 + 1079 = 14{,}345$ psi

Neglecting the variable stresses, the minimum creep rate at this stress for Hastelloy alloy X blade material from Figure XVIII is 2.3×10^{-7} in./in./hr.

Assuming the creep strain that is allowed in the turbine blades as 0.001 inches per inch and neglecting the primary creep, the useful lifetime of these blades is

$$0.001/2.3 \times 10^{-7} = 4348 \text{ hours}$$

If this is too short a period for the life of the turbine blade designed, a different material may be used possessing greater resistance to creep or the design can be changed by reducing the operating speed which in turn reduces the stress acting on these turbine blades.

Parts may be subjected to the combined bending and direct load straining action under creep conditions. When the predominant action is bending, the parts are much more favorably stressed than would be the case if the material were elastic, and the design can be based on as described by R. W. Bailey.(23) When the predominant action is a direct load, the stress conditions will approach those for elastic conditions.

(23) Bailey, R. W., "Utilization of Creep Test Data in Engineering Design," Institution of Mechanical Engineers (London), Vol. 131, 1935.

RECOMMENDATIONS AND CONCLUSIONS

Because many millions of dollars are derived from the design and assembly of equipment with an intrinsic safety factor or factor of ignorance, it would be desirable to invest more money in testing equipment that would give more accurate results in creep tests. Such tests can be applied with reliability and accuracy in design for optimum conditions. The present day equipment is enough to do the basic laboratory research in this field.

The results obtained in the experiments are satisfactory except in the case of the high minimum creep rates. In the author's experience, the difference between the exact minimum creep rate and that obtained in the experiments increased as the stress increased. This conclusion has been reached after establishing the following facts. The first fact is that the minimum creep rates are higher in a sheet than in a bar of the same material. The second fact is that the minimum creep rate which the author obtained in his experiment is less in the first test (12,500 psi), equal in the second test (25,000 psi) and higher in the third test (35,000 psi) in comparison to the data supplied by Union Carbide Corporation on a sheet of the same material. The third fact is that the minimum creep rates which were obtained in the author's experimentation all lay in one perfect straight line as shown in Figure XVIII.

In spite of the many difficulties that were experienced throughout the author's experimentation, he is happy to say that he obtained good results because the overall performance was good and the points plotted in Figure XVIII were all located on a straight line. Suggestions for improving the existing creep testing equipment at South Dakota State University would first apply to the extensometer device. Since the platinum strips are not in the same plane, the microscope cannot be focused properly on both strips at the same time. Thus either one or the other is in proper focus at any particular time.

By use of the mechanism shown in Figure XX, this difficulty can be avoided. Figure XX is an illustration of a slotted stainless steel section with a mating section designed to slide in the slotted section. One platinum strip is welded to the front face of the slotted stainless steel section and the second platinum strip is welded to the front face of the mating stainless steel section. This is a configuration in which both platinum seatings are in the same plane at all time. In order to obtain more accuracy in the measurements, an alternate slotted configuration such as a Tee slot can be investigated.

The error in the minimum creep rate is due to the manner in which the extensometer device is attached to the specimen. The effect of fillet radii and the increase in diameter due to the shoulders of the specimen can be determined in the following manner. Attach the brackets to which one set of platinum strips (instead of two sets as we did in all the tests) is welded, to the shoulders of the specimen facing one of the windows in the furnace. Form a right angle bend with each of two stainless steel wires. To one end of each of these wires, spot weld a platinum strip. After this is accomplished, weld the other end of each of these wires to the specimen under test. Other than the changes mentioned above, the configuration is the same as that previously described. The creep microscope readings can be taken from both sides of the furnace. The distance between the two welded spots on the specimen should be at least four times the diameter of the specimen. It is to be noted that the effects of fillet radii and increase in diameter due to shoulders of the specimen are avoided in this case. If we measure the creep of both different attachments, the difference between the two will give us the effects of fillet radii and increase in diameter due to the shoulders of the specimen.

The other factors like calibrating the furnace by trial and error method (as described in the furnace manual) to minimize the temperature variation along the specimen gauge length, calibrating the thermocouples accurately and using new thermocouples for each test, focusing the microscope on the same area and moving the bifilar cross hairs in the same direction to reach both reference points, standardizing the potentiometer controller circuit everyday and using new battery for each test improves the accuracy of the results.

It was also found during the first test (12,500 psi stress level) that the leveling switches in the leveling switch assembly were not sensing even when the lever was inclined more than 1°F to the horizontal. When checked once, the inclination of the lever was found as follows. The author took two points which were 8" apart on the longer arm of the lever and measured with accurate gauges the height of these two end points on the longer arm from the top of the top plate of the basic frame assembly of the creep testing machine to the bottom of the longer arm. From these measurements the angle of inclination of the lever to the horizontal is calculated in the first test and found as 1.28. Before anyone starts an experiment on this machine, better adjust the leveling switches in the leveling switch assembly as described in the manual.

If there is a creep microscope stand which can be moved horizontally and vertically with a device of ball and socket arrangement, it will be more convenient than mounting the microscope on a bracket. Also if the furnace is made in two halves with a provision to clamp them firmly together during experimentation, this arrangement would be more convenient to install the specimen in position and to focus the microscope on the platinum strips used for extension measurements.

The rupture time for Hastelloy alloy X bar material at 1200°F and 35,000 psi stress level was found by interpolation from a graph supplied by Union Carbide Corporation as round about 470 hours. The conclusion reached by the author shows that the minimum creep rates obtained in all the three tests are higher than the actual values because of the manner in which the extensometer device is attached to the specimen. The other factors like temperature variation along the specimen gauge length, the temperature variation from time to time, etc., also effect the minimum creep rate. So the rupture time for 35,000 psi stress level should be a little bit less than or at most equal to 470 hours. However, the rupture time found at 1200°F and 35,000 psi stress level was 569.1 (60 + 509.1) hours. The difference in rupture time between the value obtained in the author's experimentation and the value published by the manufacturer is at least 100 hours. The explanation for this difference is as follows:

The creep tension test at 35,000 psi stress level was carried out in two stages. The test was stopped at 60 hours, cooled rapidly at room temperature (75°F) without removing the load by sliding the furnace away from the specimen. As the specimen cooled down, the gearmotor operated automatically and brought the lever to the horizontal position, thus the load maintained constant until the specimen approximately reached the room temperature. The load was then removed, the brackets of the extensometer device to the specimen shoulders were refixed and the test continued. The way it was cooled affected and increased the time for rupture to 100 hours due to recrystallization. Apparently the material possesses the property of either increased resistance to creep or greater elongation. The other mechanical properties were not determined after cooling to room temperature in the middle of the test. If these mechanical properties satisfy the required conditions for design, the process of cooling helps in getting favorable high temperature creep properties on the same existing material. Further research can be done in improving the creep properties in this way on the existing materials as well as finding new materials which will be more creep resistant for high temperature purposes.

LITERATURE CITED

(1) Marin, Joseph (Editor), "Materials Engineering Design for High Temperatures," Department of Engineering Mechanics, The Pennsylvania State University.

(2) Finnie, I. and Heller, W. R., "Creep of Engineering Materials," McGraw Hill Book Co., Inc., New York, pp. 3, 1959.

(3) Andrade, E. N. dac., "The Viscous Flow in Metals and Allied Phenomena," Proceedings of Royal Society (London), Vol. 84, pp. 1, 1910.

(4) Finnie and Heller, op. cit., pp. 10.

(5) McVetty, P. G., "Factors Affecting the Choice of Working Stresses for High Temperature Service," Transactions of A.S.M.E., Vol. 55, pp. 99, 1933.

(6) Weaver, S. H., "The Creep and Stability of Steels at Constant Stress and Temperature," Transactions of A.S.M.E., Vol. 58, pp. 745-751, 1936.

(7) Sturm, R. G., Dumont, C., and Howell, F. M., "A Method of Analyzing Creep Data," Transactions of A.S.M.E., Vol. 58, pp. 62-67, 1936.

(8) Marin, Joseph, "Mechanical Behavior of Engineering Materials," Prentice Hall, Inc., Englewood Cliffs, N. J., 1962.

(9) Nadai, A., "The Influence of Time Upon Creep - The Hyperbolic Sine Creep Law," Stephen Timoshenko 60th Anniversary Volume, The Macmillan Company, New York, pp. 155-171, 1938.

(10) Clark, C. L., "Cooperative Creep Tests on 0.35 C Steel K20 at 85°F and 7500 Psi," Transactions of A.S.M.E., Vol. 59, pp. 439-440, 1937.

(11) American Society for Testing Materials, "Conducting of Long Time Tension Tests of Metallic Materials," A.S.T.M. Standards, Part 1, Metals, 1958.

(12) American Society for Testing Materials, "Tentative Recommended Practice for Conducting Creep and Time for Rupture Tension Tests of Materials," A.S.T.M. Standards, Part 3, pp. 274, 1961.

(13) Union Carbide, "Hastelloy Alloy-X," Union Carbide Corporation, Kokomo, Indiana, August 1961.

(14) Donachie, Mathew J., Jr., and Shepheard, Robert G., "Creep Rupture Behavior of Hastelloy X," A.S.T.M. Proceedings, Vol. 61, pp. 981, 1961.

(15) Tapsell, H. J., "Creep of Metals," Oxford University Press, London, 1931.

(16) Emmert, H. D., "Current Design Practices for Gas Turbine Power Elements," Transactions of A.S.M.E., Vol. 72, pp. 189, February 1950.

(17) Weaver, op. cit., pp. 745-751.

(18) Lee, John F., "Theory and Design of Steam and Gas Turbines," McGraw Hill Book Company, Inc., New York, 1954.

(19) Seely, Fred B., Ensign, Newton E., Jones, Paul G., "Analytical Mechanics for Engineers," John Wiley & Sons, Inc., New York, 1958.

(20) Sorensen, Harry A., "Gas Turbines," Ronald Press, New York, 1958.

(21) Emmert, op. cit., pp. 197.

(22) Emmert, op. cit., pp. 197.

(23) Bailey, R. W., "Utilization of Creep Test Data in Engineering Design," Institution of Mechanical Engineers (London), Vol. 131, 1935.

(24) Crout, Prescot D., "A Short Method for Evaluating Determinants and Solving Systems of Linear Equations with Real or Complex Coefficients," Transactions of A.S.E.E., Vol. 60, pp. 1235, 1941.

APPENDIX A

PROPERTIES OF HASTELLOY ALLOY X

Chemical Composition, Percent

Nickel	Cobalt	Chromium	Molybdenum	Tungsten	Iron	Carbon	Silicon	Manganese
Bal-ance	0.5 to 2.5	20.5 to 23.0	8.0 to 10.0	0.2 to 1.0	17.0 to 20.0	0.05 to 0.15	1.0*	1.0*

The bar is solution heat treated at 2175°F according to the specification: AMS 5754 - C, and then water quenched.

Melting temperature = 2350°F

Density = 0.297 lb./cu.in.

Mean coefficient of thermal expansion (79 - 1200°F) = 8.56 micro inches/inch/degree F

Specific heat = 0.105 BTU/lb.-deg. F

Modulus of elasticity at room temperature = 28.49×10^6 psi

Modulus of elasticity at 1200°F = 22.32×10^6 psi approximately

This material is a nickel base alloy with exceptional strength and oxidation resistance up to 2200°F and also has forming and welding characteristics.

Further details on this material can be obtained from Haynes Stellite division, Union Carbide Corporation, Kokomo, Indiana.

*Maximum values.

APPENDIX B

METHOD OF LEAST SQUARES

The proposed equation for the experimental data is

log(creep strain) = a + b log(time)

or $\bar{c}_k = a + b\,\bar{t}_k$

Suppose the creep strain that we get after determining and using the constants 'a' and 'b' is c_{1k} for any time 't_k'.

The principle employed in this method is to minimize the error $(\bar{c}_k - \bar{c}_{1k})$ by making the sum of the squares of the residuals $(\bar{c}_k - \bar{c}_{1k})$ as small as possible.

The sum to be minimized is $\sum_{k=1}^{n}(\bar{c}_k - \bar{c}_{1k})^2 = \sum_{k=1}^{n}\left[\bar{c}_k - (a + b\,\bar{t}_k)\right]^2$

$$= \sum_{k=1}^{n}\bar{c}_k^2 + n\,a^2 + b^2\sum_{k=1}^{n}t_k^2 - 2a\sum_{k=1}^{n}\bar{c}_k - 2b\sum_{k=1}^{n}\bar{c}_k\,\bar{t}_k + 2ab\sum_{k=1}^{n}\bar{t}_k$$

Where n = number of observations.

To determine 'a' and 'b' which will make $\sum_{k=1}^{n}(\bar{c}_k - \bar{c}_{1k})^2$ a minimum, the partial derivatives with respect to 'a' and 'b' must be equal to zero.

i.e., $$\frac{\partial}{\partial a}\sum_{k=1}^{n}\left[(\bar{c}_k - \bar{c}_{1k})^2\right] = 2na - 2\sum_{k=1}^{n}\bar{c}_k + 2b\sum_{k=1}^{n}\bar{t}_k = 0$$

or $$a = \frac{\sum_{k=1}^{n}\bar{c}_k}{n} - b\,\frac{\sum_{k=1}^{n}\bar{t}_k}{n} = A\bar{c}_k - bA\bar{t}_k \qquad (6)$$

where $A\bar{c}_k = \frac{\sum_{k=1}^{n}\bar{c}_k}{n}$ (the average of the c_k's) and $$\frac{\partial}{\partial b} \sum_{k=1}^{n}\left[(\bar{c}_k - \bar{c}_{1k})^2\right] = 2b\sum_{k=1}^{n}\bar{t}_k^2 - 2\sum_{k=1}^{n}\bar{c}_k\bar{t}_k + 2a\sum_{k=1}^{n}\bar{t}_k = 0$$

or $$b\sum_{k=1}^{n}\bar{t}_k^2 - \sum_{k=1}^{n}\bar{c}_k\ \bar{t}_k + \left[\frac{\sum_{k=1}^{n}\bar{c}_k}{n} - b\frac{\sum_{k=1}^{n}\bar{t}_k}{n}\right]\sum_{k=1}^{n}\bar{t}_k = 0$$

i.e., $$b\sum_{k=1}^{n}\bar{t}_k^2 - \sum_{k=1}^{n}\bar{c}_k\ \bar{t}_k + n\ A\bar{c}_k\ A\bar{t}_k - nb\ (A\bar{t}_k)^2 = 0$$

or $$b\sum_{k=1}^{n}\left[\bar{t}_k^2 - n(A\bar{t}_k)^2\right] = \sum_{k=1}^{n}\bar{c}_k\ \bar{t}_k - n\ A\bar{c}_k\ A\bar{t}_k$$

$$b = \frac{\sum_{k=1}^{n}\bar{c}_k\ \bar{t}_k - n\ A\bar{c}_k\ A\bar{t}_k}{\sum_{k=1}^{n}\bar{t}_k^2 - n(A\bar{t}_k)^2}$$

APPENDIX C

PRINCIPLE OF LEAST SQUARES TO FIT WITH POLYNOMIAL EQUATION

The proposed polynomial expression to fit the experimental data of 25,000 psi stress level is $= a_o + a_1 t + a_2 t^2 = \sum_{i=0}^{2} a_i t^i$.

$$\in_1 = a_o + a_1 t_1 + a_2 t_1^2$$

$$\in_2 = a_o + a_1 t_2 + a_2 t_2^2$$

.... = ...

.... = ...

$$\in_k = a_o + a_1 t_k + a_2 t_k^2$$

The principle of least squares states that the best representation of the data is that which makes the sum of the squares of the differences between the calculated values and the observed values a minimum. That is

$$(a_o+a_1 t_1+a_2 t_1^2- \in_1)^2+(a_o+a_1 t_2+a_2 t_2^2- \in_2)^2+\ldots\ldots+(a_o+a_1 t_k+a_2 t_k^2- \in_k)^2$$

$$= F\ (a_o,\ a_1,\ a_2) \text{ must be minimum.}$$

To satisfy this condition, the partial derivatives with respect to 'a_o', 'a_1' and 'a_2' must be zero. That is,

$$\frac{\partial F}{\partial a_o}=2(a_o+a_1 t_1+a_2 t_1^2- \in_1)+(a_o+a_1 t_2+a_2 t_2^2- \in_2)+\ldots+(a_o+a_1 t_k+a_2 t_k^2- \in_k)=0$$

$$\frac{\partial F}{\partial a_1}=2(a_o+a_1 t_1+a_2 t_1^2- \in_1)t_1+(a_o+a_1 t_2+a_2 t_2^2- \in_2)t_2+\ldots+(a_o+a_1 t_k+a_2 t_k^2- \in_n)t_k=0$$

$$\frac{\partial F}{\partial a_2}=2(a_o+a_1 t_1+a_2 t_1^2- \in_1)t_1^2+(a_o+a_1 t_2+a_2 t_2^2- \in_2)t_2^2+\ldots+(a_o+a_1 t_k+a_2 t_k^2- \in_n)t_k^2=0$$

or

$$na_o+a_1(t_1+t_2+t_3+...+t_k)+a_2(t_1^2+t_2^2+...+t_k^2)= \epsilon_1+ \epsilon_2+...+ \epsilon_k$$

$$a_o(t_1+t_2+t_3+...+t_k)+a_1(t_1^2+t_2^2+...+t_k^2)+a_2(t_1^3+t_2^3+...+t_k^3)= \epsilon_1 t_1+ \epsilon_2 t_2+...+ \epsilon_k t_k$$

$$a_o(t_1^2+t_2^2+...+t_k^2)+a_1(t_1^3+t_2^3+...+t_k^3)+a_2(t_1^4+t_2^4+...+t_k^4)= \epsilon_1 t_1^2+ \epsilon_2 t_2^2+...+ \epsilon_k t_k^2$$

or

$$S_o\ a_o + S_1\ a_1 + S_2\ a_2 = K_o \text{ ------------ } (1)$$

$$S_1\ a_o + S_2\ a_1 + S_3\ a_2 = K_1 \text{ ------------ } (2)$$

$$S_2\ a_o + S_3\ a_1 + S_4\ a_2 = K_2 \text{ ------------ } (3)$$

where $S_o = t_1^o + t_2^o +...+ t_k^o = n$

$$S_1 = t_1 + t_2 + t_3 +....+ t_k = \sum_{k=1}^{n} t_k$$

$$S_2 = t_1^2 + t_2^2 +....+ t_k^2 = \sum_{k=1}^{n} t_k^2$$

$$S_3 = t_1^3 + t_2^3 +....+ t_k^3 = \sum_{k=1}^{n} t_k^3$$

$$S_4 = t_1^4 + t_2^4 +....+ t_k^4 = \sum_{k=1}^{n} t_k^4$$

$$K_o = \epsilon_1 + \epsilon_2 +....+ \epsilon_k = \sum_{k=1}^{n} \epsilon_k$$

$$K_1 = \epsilon_1 t_1 + \epsilon_2 t_2 +....+ \epsilon_k t_k = \sum_{k=1}^{n} \epsilon_k t_k$$

$$K_2 = \epsilon_1 t_1^2 + \epsilon_2 t_2^2 +....+ \epsilon_k t_k^2 = \sum_{k=1}^{n} \epsilon_k t_k^2$$

The linear equations (1), (2) and (3) are known as normal equations. These equations can be solved by Crout's[24] Method.

From the matrix of the system plus a check column

$$\begin{vmatrix} S_0 & S_1 & S_2 & K_0 & F_1 \\ S_1 & S_2 & S_3 & K_1 & F_2 \\ S_2 & S_3 & S_4 & K_2 & F_3 \end{vmatrix}$$

where

$$F_1 = S_0 + S_1 + S_2 + K_0$$

$$F_2 = S_1 + S_2 + S_3 + K_1$$

$$F_3 = S_2 + S_3 + S_4 + K_2$$

A derived matrix

$$\begin{vmatrix} A_1 & B_1 & C_1 & D_1 & E_1 \\ A_2 & B_2 & C_2 & D_2 & E_2 \\ A_3 & B_3 & C_3 & D_3 & E_3 \end{vmatrix}$$

can be calculated in the following manner.

Step 1: First column, $A_1 = S_0$, $A_2 = S_1$, $A_3 = S_2$

Step 2: First row, $B_1 = S_1/S_0$, $C_1 = S_2/S_0$, $D_1 = K_0/S_0$, $E_1 = F_1/S_0$

Check: $E_1 = 1 + B_1 + C_1 + D_1$

Step 3: Second column, $B_2 = S_2 - B_1 A_2$, $B_3 = S_3 - B_1 A_3$

---

[24] Crout, Prescot D., "A Short Method for Evaluating Determinants and Solving Systems of Linear Equations with Real or Complex Coefficients," Trans. A.I.E.E., Vol. 60, pp. 1235, 1941.

Step 4: Remaining second row, $C_2 = \dfrac{S_3 - C_1A_2}{B_2}$; $D_2 = \dfrac{K_1 - D_1A_2}{B_2}$

$$E_2 = \frac{F_2 - E_1A_2}{B_2}$$

Check: $E_2 = 1 + C_2 + D_2$

Step 5: Remaining third column, $C_3 = S_4 - C_2B_3 - C_1A_3$

Step 6: Remaining third row,

$$D_3 = \frac{K_2 - D_2B_3 - D_1A_3}{C_3}$$

$$E_3 = \frac{F_3 - E_2B_3 - E_1A_3}{C_3}$$

Check: $E_3 = 1 + D_3$

Solutions are then given by:

$$a_2 = D_3$$

$$a_1 = D_2 - C_2a_2$$

$$a_o = D_1 - C_1a_2 - B_1a_1$$